



# Deformation along the Deseado Massif (Patagonia, Argentina) during the Jurassic Period and its relationship with the Gondwana breakup: paleomagnetic and geochronological constraints

V. Ruiz González <sup>a,\*</sup>, E.M. Renda <sup>b</sup>, H. Vizán <sup>a</sup>, M. Ganerød <sup>c</sup>, C.G. Puigdomenech <sup>a</sup>, C.B. Zaffarana <sup>b</sup>

<sup>a</sup> Instituto de Geociencias Básicas, Aplicadas y Ambientales de Buenos Aires (IGEBA, CONICET-UBA), Intendente Güiraldes 2160, C1428EHA Ciudad Autónoma de Buenos Aires, Argentina

<sup>b</sup> Instituto de Investigación en Paleobiología y Geología (IIPG, CONICET-UNRN), Av. Roca 1242, General Roca, Río Negro, Argentina

<sup>c</sup> Geological Survey of Norway, Leiv Erikssonsvei 39, 7040 Trondheim, Norway

## ARTICLE INFO

### Keywords:

Jurassic  
Deseado Massif  
Patagonia  
Gondwana  
Paleomagnetism  
<sup>40</sup>Ar–<sup>39</sup>Ar dating

## ABSTRACT

This work presents the analysis of paleomagnetic results obtained from four sampling areas of the Jurassic Bahía Laura Complex in the Deseado Massif and their implications on the regional deformation history during the breakup of Gondwana. Paleomagnetic data show cessation of tectonic block rotations about vertical axes around 160 Ma and a change from a transtensional to a mainly extensional tectonic regime. Two biotite samples yielded <sup>40</sup>Ar–<sup>39</sup>Ar radiometric ages: one from the eastern outcrops of the Chon Aike Formation (plateau age of 184.66 ± 0.55 Ma) and the other from the La Matilde Formation (plateau age of 157.40 ± 0.65 Ma), located at the central part of the Deseado Massif. Finally, an apparent polar wander path (APWP) was calculated for the Jurassic of South America (200 to 140 Ma). This APWP indicates that South America experienced a northward drift between 200 Ma and 170 Ma, a clockwise rotation (~10°) between 170 Ma and 160 Ma, and a westward drift between 160 Ma and 140 Ma. The 170–160 Ma rotation could have been triggered by the combined effects of the uncoupling of the Antarctic Peninsula, the high rates of subduction of the Phoenix plate beneath Patagonia, the opening of the Rocas Verdes basin and the Weddell Sea, and the cessation of the Tethys slab-pull. Furthermore, the calculated APWP for South America does not support a Jurassic massive true polar wander event.

## 1. Introduction

The Deseado Massif (DM), a geological province located in southern Patagonia within the Santa Cruz Province (Argentina), shows a well-preserved geological record since early Paleozoic times (Fig. 1), which represents a key element to unravel the Gondwana breakup. This massif is bounded by the Deseado River to the north, the Chico River to the south, the Atlantic Ocean to the east, and the Cenozoic sedimentary successions from the Andean foreland basins to the west (e.g., Fernández et al., 2016; Giacosa et al., 2002; Guido, 2004; Martino et al., 2020; Moreira et al., 2009; Páez et al., 2016). The denomination of this geological province has been an object of discussion because of its tectonostratigraphic complexity. It was originally proposed as an independent lithospheric massif (Feruglio, 1946), named Deseado Massif (Leanza, 1958). Later on, Harrington (1962) recognized it as an area of

sub-stable, sub-positive, undeformable units separated from the cratons by negative belts (as is the case of the San Jorge Gulf Basin with respect to the North Patagonian and Deseado massifs), and defined it as the “Deseado Nesocraton”. Afterward, due to the thickness of the Late Paleozoic–Mesozoic sedimentary units deposited in the DM, Homovc and Constantini (2001) called it the “Deseado Basin”. The latest name given to the DM was proposed by Fracchia and Giacosa (2006), calling it the “Deseado Region” and discarding the definition of massif. In this work, we maintain the original naming of Deseado Massif due to its own crustal and geophysical characteristics (Ferpozzi and Johanis, 2004; Ramos, 1999).

Since the Triassic period, the overall tectonic regime along Pangea was extensional, which triggered the formation of the accommodation space of the Mesozoic basins and, finally, the supercontinent breakup (e.g., Vizán et al., 2017). In Gondwana, this extensional regime could be

\* Corresponding author.

E-mail address: [vruizgonzalez@gl.fcen.uba.ar](mailto:vruizgonzalez@gl.fcen.uba.ar) (V. Ruiz González).

related with the collapse of the Godwanides (e.g., Kern et al., 2021; Ramos, 2008), the later opening of the Weddell Sea and the Rocas Verdes Basin during the Early-Middle Jurassic (e.g., Bastias et al., 2021; Calderón et al., 2007; Cao et al., 2022; Dalziel et al., 1974; Ferris et al., 2000; Ghidella et al., 2002; Grunow, 1993; Grunow et al., 1987; Jordan et al., 2017, 2020; König and Jokat, 2006; Riley et al., 2020; Suárez et al., 2019), and finally with the opening of the South Atlantic Ocean since the Early Cretaceous (e.g., Creer et al., 1972; Eagles, 2007; Nürnberg and Müller, 1991; Schult and Guerreiro, 1979; Torsvik et al., 2009). Furthermore, the regional crustal thinning and the associated uplift of the asthenosphere (e.g., Huang et al., 2019; Zhong et al., 2007), aided in the formation of Large Igneous Provinces such as the felsic Chon Aike Igneous Province (198–145 Ma; Kay et al., 1989), the mafic Paraná-Etendeka Magmatic Province (130–132 Ma; Renne et al., 1992) and the Central Atlantic Magmatic Province (190–202 Ma; May, 1971).

After this period of regional extension, the tectonic regime changed during the mid-Cretaceous, and a compressional tectonic regime started in the studied region, triggering the development of the Andean orogeny (Somoza and Zaffarana, 2008). This orogeny caused the partial inversion of extensional Jurassic structures and the reactivation of Paleozoic

structures (e.g., Giacosa et al., 2010; Japas, 2001; Japas et al., 2013; Navarrete, 2021; Renda et al., 2019).

During Late Triassic to Early Jurassic times, a major displacement of the southern part of Patagonia (including the DM) was proposed implying a movement of 500 km towards the west, from a near South Africa position to its current location with respect to South America (Rapela and Pankhurst, 1992). Several authors have widely invoked this longitudinal displacement in their paleogeographic reconstructions (e.g., Dalziel et al., 2000; Hole et al., 2016; Jordan et al., 2020; Macdonald et al., 2003; Marshall, 1994; Storey et al., 1992; Torsvik et al., 2008). However, other authors refute the displacement of the southern part of Patagonia at that time, according to the multidisciplinary analysis (paleomagnetism, anisotropy of magnetic susceptibility, petrology, structural geology) of the structures and features linked with this event (von Gosen and Loske, 2004; Renda et al., 2019; Ruiz González et al., 2020; Zaffarana et al., 2010; Zaffarana et al., 2014, 2017; Zaffarana et al., 2012; Zaffarana and Somoza, 2012).

Due to the complex and discussed geological history of the DM, the main objective of this work is to integrate field observations with paleomagnetic and geochronological data in order to analyze the

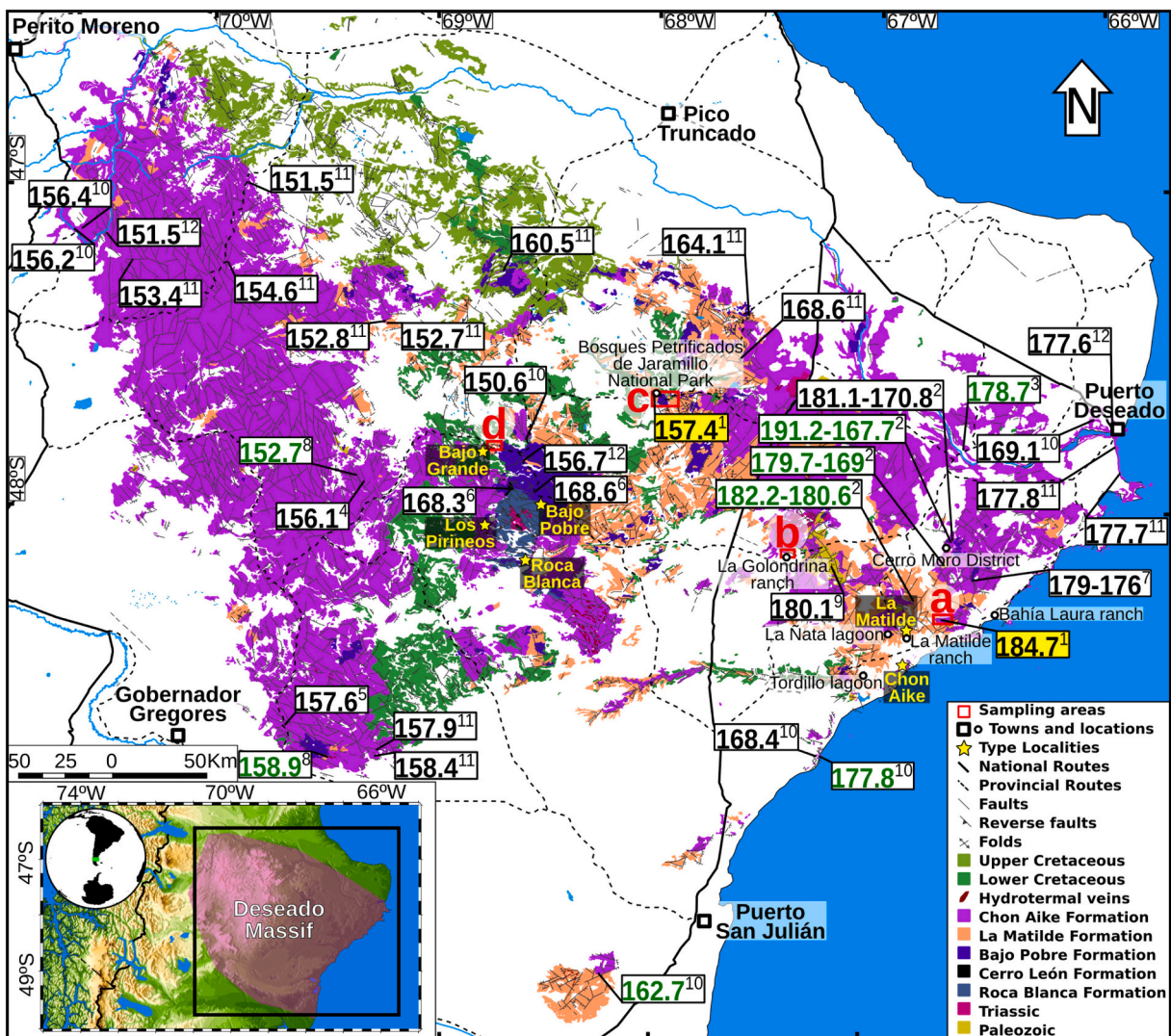


**Fig. 1.** Map of the Deseado Massif (modified from Panza et al., 2003), with the sampling areas highlighted with a red square (see Fig. 2). Cenozoic units are omitted. Also, reliable Jurassic radiometric ages are presented: 1) this work, 2) Matthews et al. (2021), 3) Navarrete et al. (2020), 4) Ruiz González et al. (2019), 5) Páez et al. (2016), 6) Jovic (2010), 7) Guido et al. (2006), 8) Moreira et al. (2006), 9) Guido et al. (2004), 10) Pankhurst et al. (2000), 11) Féraud et al. (1999), 12) Alric et al. (1996). Ages determined by the Ar–Ar method are shown in black and those determined by the U–Pb method are shown in green. (For interpretation of the references to colour in this figure legend, the reader is referred to the web version of this article.)

deformation recorded in the units of the Jurassic Bahía Laura Complex. Also, this work aims to deduce the shape and paleogeography of this massif with respect to the rest of Patagonia, South America, and southwestern Gondwana during Jurassic times. Therefore, the previous tectonic and paleogeographic proposals about the DM will be discussed.

## 2. Geological framework

### 2.1. Stratigraphic units

The Jurassic volcano-sedimentary units of the Bahía Laura Complex and the sedimentary and volcanic Cenozoic units, cover most of the DM along with scattered outcrops of Paleozoic, Triassic, and Cretaceous units (Fig. 1). The oldest unit in the DM is the Ordovician (Moreira et al., 2013) La Modesta Formation (Di Persia, 1962), cropping out in the western part of the massif. Mid-Paleozoic units are present in the eastern part of the DM, where the Silurian-Devonian (Pankhurst et al., 2003) mid- to high-grade metamorphic units of the Río Deseado Complex crop out (Viera and Pezzuchi, 1976). These are covered by the Permian sedimentary units of La Golondrina (Archangelsky, 1967) and La Juanita (Arrondo, 1972) formations (Fig. 1).

The first Mesozoic stratigraphic unit in the DM is the Triassic sedimentary succession of the El Tranquilo Group (Di Persia, 1955; Jalfin and Herbst, 1995). This group is intruded in the eastern part of the DM by granites of the Upper Triassic (Navarrete et al., 2019; Pankhurst et al., 1993) La Leona Formation (Arrondo, 1972). The Jurassic Period is represented, from bottom to top, by the Roca Blanca (Herbst, 1965), Cerro León (Pezzi, 1970), Bajo Pobre (Turic, 1969), La Matilde and Chon Aike (Stipanicic and Reig, 1957) volcano-sedimentary formations. These last four formations constitute the Bahía Laura Complex (Feruglio, 1949). In the central part of the DM, the sedimentary Bajo Grande Formation (Di Persia, 1958) lies in angular unconformity over the Bahía Laura Complex, and it underlies in angular unconformity the sedimentary units of the Baqueró Group from the Lower Cretaceous (Cladera et al., 2002). The last Mesozoic units of the DM are the Upper Cretaceous sedimentary units of the Chubut Group (Lesta and Ferello, 1972).

### 2.2. Structural features

The lithostratigraphic units of the DM record a complex tectonic evolution consisting of different deformational phases. Each phase produced a different set of structural features, aiding in their identification and correlation (e.g., Giacosa et al., 2010, and references therein). The deformation caused by the Paleozoic regional tectonism left several major structures, which conditioned the subsequent deformation throughout Patagonia (e.g., Navarrete, 2021; Renda et al., 2019; Uliana and Biddle, 1987). Faults and fractures are the main features formed during the Jurassic and Early Cretaceous in the DM (Fig. 1), allowing the identification of different crustal tectonic blocks that formed grabens and half-grabens with normal and horizontal shear displacements (Giacosa et al., 2010; Homovc and Constantini, 2001; Japas et al., 2013; Reimer et al., 1996). Japas et al. (2013) divided the faults and fractures on the Jurassic units into two main sets: Population A (principal), indicating a direction of major extension between ENE and NE (main kinematic axes azimuth: 130°–160°), and a younger Population B (secondary), indicating a direction of major extension between NNW and NW (main kinematic axes azimuth: 35°–85°).

During the late Early Cretaceous, some of the previous extensional structural features were reactivated as reverse faults due to the tectonic inversion triggered by the compressive stresses of the Andean orogeny (e.g., Giacosa et al., 2010). These N-S reverse faults located in the central part of the DM (see Fig. 1) are considered by Japas et al. (2013) as the limit between the eastern and western domains of the DM, also proposed as part of the Patagonian Broken Foreland by Bilmes et al. (2013). Likewise, some late Early Cretaceous minor folds are reported, mainly in the central part of the DM (Giacosa et al., 2010; Panza, 1982, 1984;

Fig. 1).

### 2.3. Sampling sites

Paleomagnetic sampling was carried out in four areas comprising the surroundings of the Bahía Laura bay, 17 km to the west of the Bahía Laura ranch, to the Bajo Grande topographic depression, in the central part of the DM (Fig. 1). All lithostratigraphic units studied in this work belong to the Bahía Laura Complex: Chon Aike (Figs. 2a and b), Bajo Pobre (Fig. 2c) and La Matilde (Fig. 2d) formations.

The Jurassic silicic volcanic flare-up of the Chon Aike Igneous Province (Kay et al., 1989) is well preserved in the outcrops of the Chon Aike Formation (Cobos et al., 2003; Escosteguy et al., 2003; Giacosa et al., 2001; Giacosa and Genini, 1998; Panza et al., 1994a, 1994b, 1998, 2001a, 2001b, 2018; Panza and Márquez, 1994). The units that form the Chon Aike Formations type locality, near the Atlantic coast (Fig. 1), are reddish, purplish, and greenish colored porphyritic rhyolites, rhyolitic tuffs, and acid volcanic breccias (Stipanicic and Reig, 1955, 1957). This lithological association is widely distributed throughout the DM and comprises regional-scale ignimbritic plateaus, isolated domes, dikes, and rhyolitic to dacitic lava flows (Archangelsky, 1967; De Giusto et al., 1980; Echavarría, 1999; Fernández et al., 2016; Guido, 2004; Herbst, 1965; Moreira et al., 2009; Navarrete et al., 2020, 2021; Sruoga and Palma, 1984, 1986; Sruoga et al., 2008). In this work, the Chon Aike Formation was sampled in two areas in the eastern part of the DM (Fig. 1). One area near the Bahía Laura bay, 17 km to the west of the Bahía Laura ranch (Fig. 1). Here the outcrops form brown-purplish mounds of orange to gray-purplish welded rhyolitic to dacitic tuffaceous units. A rock sample for  $^{40}\text{Ar}$ — $^{39}\text{Ar}$  dating was also collected from a grayish dacitic ignimbrite at the CA06 site (see the star in Fig. 2a). In the second sampling area, near the La Golondrina ranch (Fig. 2b), the outcrops of the Chon Aike Formation show greater lithological diversity than those near Bahía Laura bay. These rocks vary between rheomorphic ignimbrites and ignimbritic breccias, rhyolitic-dacitic lava-like flows, and rhyolitic pyroclastic dykes (tuffisites). These units are similar to those described by Navarrete (2021) and Navarrete et al. (2020, 2021), linked to fissural eruptions.

The Bajo Pobre Formation (Fig. 2c) comprises basaltic to andesitic rocks (Lesta and Ferello, 1972; Pezzi, 1970; Turic, 1969). The typical lithologic succession of this formation consists of a lower massive section with marked columnar jointing and an upper vesicular or amygdaloidal section (Jovic, 2010). East of the Bosques Petrificados de Jaramillo National Park, the outcrops of this formation form black to purple mounds, among which are a few composed of basaltic and andesitic lavas and andesitic breccias (Panza et al., 2001a, 2001b). Dark purple and dark gray lavas were sampled from these outcrops which have an approximate extension of 9 km<sup>2</sup> (Panza et al., 2001a, 2001b; see Fig. 2c).

The last studied unit is the La Matilde Formation, first described by Stipanicic and Reig (1955) in the outcrops north of the eponymous ranch, close to the Atlantic coast (Fig. 1). This formation is composed of white-grayish and white-brownish tuffs and fluvial-lacustrine sedimentary deposits in its type locality. There, the units present their characteristic Middle Jurassic anuran fossils (Panza and Márquez, 1994, and references therein). On the other hand, in the central part of the DM, the lithologies assigned to the La Matilde Formation are composed fundamentally of white-yellowish to white-greenish tuffs and fine-grained sandstones (Panza et al., 2001a, 2001b). Furthermore, in the Bosques Petrificados de Jaramillo National Park (Fig. 2c), the units of this formation contain petrified araucaria cones and logs of Middle Jurassic age (Kloster and Gnaedinger, 2018). Also, in the Bajo Grande area (Fig. 2d), these units are composed of the same lithologies as those in the National Park, but they do not contain any fossil remains (Archangelsky, 1967; Di Persia, 1955). The La Matilde Formation in the Bosques Petrificados de Jaramillo National Park (Fig. 2c) and the topographic depression of Bajo Grande (Fig. 2d) were sampled, drilling white-yellowish tuffs and

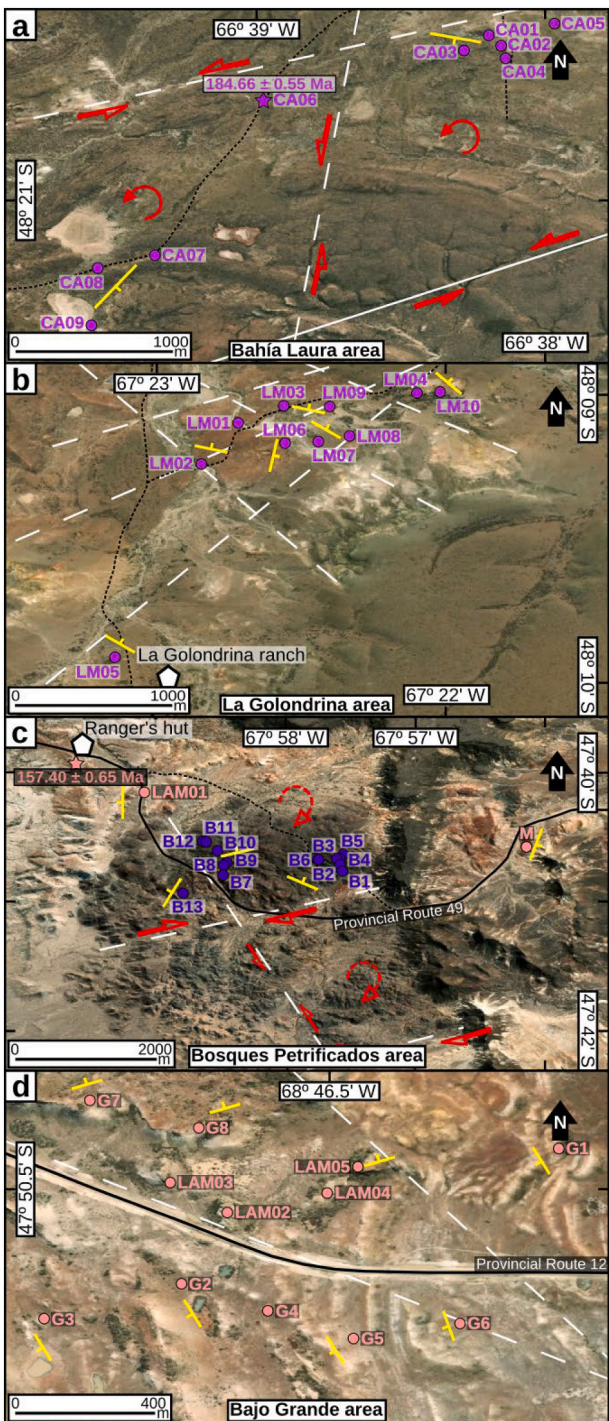


**Fig. 2.** Aerial view of the sampling areas: (a) sites of the Chon Aike Formation (purple circles and a star pointing the dated sample) near Bahía Laura bay; (b) sites of the Chon Aike Formation (purple circles) near the La Golondrina ranch; (c) sites of the Bajo Pobre and La Matilde formations (dark blue circles and light orange circles, respectively, and a star pointing the dated sample) in the Bosques Petrificados de Jaramillo National Park; (d) sites of the La Matilde Formation (light pink circles) in the topographic depression of Bajo Grande. Inferred faults are marked with discontinuous white lines, and visible faults are marked with white solid lines. In addition, the inferred slip senses and block rotations are marked with red arrows. The strike and dip of the units are shown with yellow lines. Routes and roads are marked with continuous and discontinuous black lines, respectively. (For interpretation of the references to colour in this figure legend, the reader is referred to the web version of this article.)

pyroclastic deposits with abundant biotite crystals. A rock sample for dating was also taken from a tuff underlying the layer with trunks from the National Park (see the star in Fig. 2c).

### 3. $^{40}\text{Ar}$ — $^{39}\text{Ar}$ geochronology

The Chon Aike and La Matilde formations were dated in the  $^{40}\text{Ar}$ — $^{39}\text{Ar}$  Laboratory of the Norwegian Geological Survey in Trondheim, obtaining the results from biotite grains. Raw dating data are in Supplementary Data, Table B. A sample of the Chon Aike Formation from the eastern part of the Deseado Massif (Fig. 2a) was taken from a welded grayish dacitic tuff (CA06) with millimetric crystals, lithic fragments and biotite crystals smaller than 1 mm. This sample was located near a road 17 km to the west of the Bahía Laura ranch in the Bahía Laura Bay ( $48.34410^\circ\text{S}$ ,  $66.64950^\circ\text{W}$ ; see Fig. 2a). The  $^{40}\text{Ar}$ — $^{39}\text{Ar}$  plateau indicates an age of  $184.66 \pm 0.55$  Ma (61.88% of  $^{39}\text{Ar}$  released in 11/23 steps, MSWD = 1.34; Fig. 3a) and the inverse isochron an age of  $184.81 \pm 1.37$  Ma (MSWD = 1.48; Fig. 3b).

The sample of the La Matilde Formation was collected close to the ranger's hut ( $47.66711^\circ\text{S}$ ,  $67.99613^\circ\text{W}$ ; see Fig. 2c) near one of the fossil logs of the Bosques Petrificados de Jaramillo National Park (Fig. 2c), specifically from a yellow-green rhyolitic tuff that contains the fossils of araucaria. In this unit, the biotite crystals are up to 1.5 mm and do not show corrosion edges, which facilitated subsequent separation. A plateau age of  $157.40 \pm 0.65$  Ma in  $^{40}\text{Ar}$ — $^{39}\text{Ar}$  (97.75% of  $^{39}\text{Ar}$  released in 24/25 steps, MSWD = 0.367; Fig. 3c), and an inverse isochron age of  $157.51 \pm 0.733$  Ma (MSWD = 0.37; Fig. 3d) were determined.

### 4. Paleomagnetic methods and results

From 46 sites, 304 paleomagnetic samples were drilled, taking 5 to 13 rock cylinders (samples) per site. Every sample was obtained with a hand-drilling machine and oriented with magnetic and sun compasses (when the Sun could cast a shadow). Each sample was sliced into two or more specimens. All directions were corrected by the declination of the Earth's magnetic field at the moment of the collection.

The paleomagnetic samples were demagnetized by thermal or alternating magnetic fields (AF) methods, applying progressively higher temperatures or bigger AF until the samples were utterly demagnetized (Butler, 1992). Demagnetization by AF was performed as a pilot test at every site, but the preferred method was thermal demagnetization. The experimental procedure was carried out in the Paleomagnetism Laboratory 'Daniel A. Valencio' at the University of Buenos Aires. The thermal demagnetization of the samples was performed with a TD-48 SC thermal demagnetizer of the ASC Scientific brand. For AF demagnetization, a rotating demagnetizer by alternating magnetic fields LDA-3A of AGICO brand was used, and a JR6 rotating magnetometer of AGICO brand was used for the remanence measurements. A 2G brand superconducting magnetometer with SQUID-DC SSR sensors was also used for AF demagnetization, with an automatic measurement system and integrated equipment for demagnetization by alternating currents. Only characteristic remanent magnetizations (ChRM) calculated by averaging at least three demagnetization steps and a maximum angular deviation less than  $15^\circ$  were accepted (Kirschvink, 1980). Also, thermomagnetic curves (susceptibility vs. T) were performed with CL3 and CLS attachments for the AGICO MFK1A susceptibilitymeter. These curves indicate that the possible carriers of the magnetic remanence in the ignimbritic units are titanomagnetite and hematite (Fig. 4; Dunlop and Özdemir, 1997).

#### 4.1. Chon Aike Formation

##### 4.1.1. Bahía Laura Bay Area

As presented above, an  $^{40}\text{Ar}$ — $^{39}\text{Ar}$  age was obtained from biotite, yielding an age of  $184.66 \pm 0.55$  Ma (see Fig. 1). All samples obtained from the rhyolitic and dacitic ignimbrites in the Bahía Laura bay area

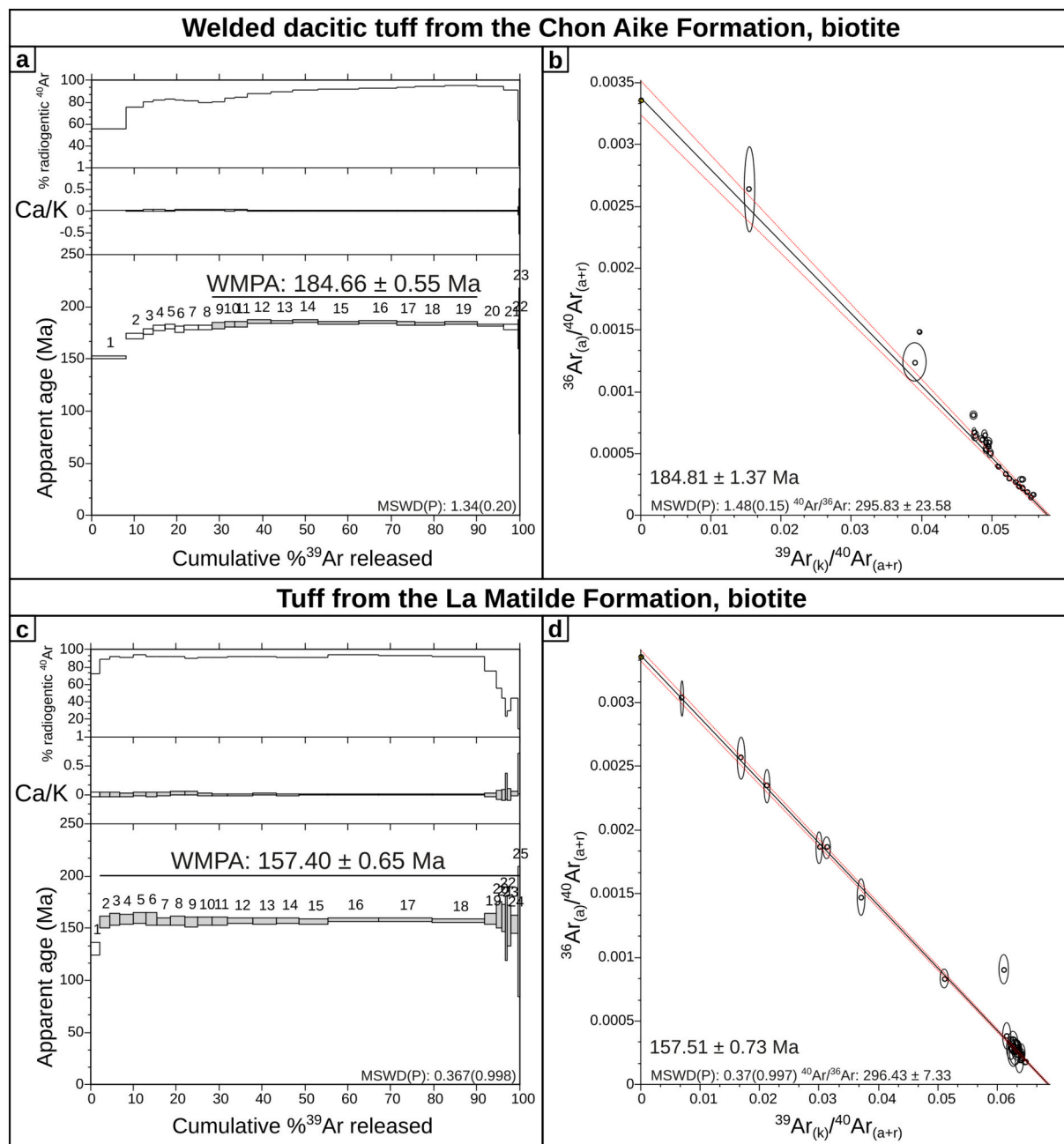


**Fig. 3.** Graphical representations of the  $^{40}\text{Ar}-^{39}\text{Ar}$  datings: (a) degassing diagram and (b) isochron diagram of the sample taken near the route 17 km to the west of Bahía Laura ranch; (c) degassing diagram and (d) isochron diagram of the sample from the La Matilde Formation taken in the Bosques Petrificados de Jaramillo National Park.

have remanence directions defined with high precision and high coercivity or unblocking temperatures (Fig. 5a). In all the samples analyzed, a ChRM was determined between  $330^\circ\text{C}$  and  $600-680^\circ\text{C}$ , or between 5 and 10 mT and 40–80 mT (A component). The bulk susceptibility changes did not condition the determination of ChRMs in every thermal demagnetization step (bulk susceptibility data are in Supplementary Data, Table A). The ChRMs obtained show reverse (positive inclination) and normal (negative inclination) polarities (Fig. 5a).

The mean directions of ChRM were calculated with six to nine samples for each sampling site (Fig. 6a). A reversal test was carried out to validate the results, giving a positive (B) result with a critical angle of  $6.9^\circ$  and an observed angle of  $4.8^\circ$  (McFadden and McElhinny, 1990). In addition, a fold test (McFadden, 1990) was calculated and the result was not statistically significant, although positive. In addition, a virtual

geomagnetic pole (VGP) was calculated from each ChRM mean direction (Table 1). Finally, a paleomagnetic pole for the Chon Aike Formation near Bahía Laura bay was obtained using the VGPs from the tilt corrected directions (Table 2).

#### 4.1.2. La Golondrina Ranch Area

The age of these units ( $\sim 180$  Ma; Fig. 1) is assumed to be close to the U—Pb ages of zircon presented by Matthews et al. (2021) and Navarrete et al. (2020) obtained from units that crop out 50 km to the east and 70 km to the northeast, respectively, with very similar lithological and structural features. The ChRM directions obtained from the samples of rhyolitic ignimbrites and breccias were defined between 270 and  $330^\circ\text{C}$  and  $630-680^\circ\text{C}$  (Fig. 5b). The changes in bulk susceptibility did not condition the determination of the ChRMs in every thermal

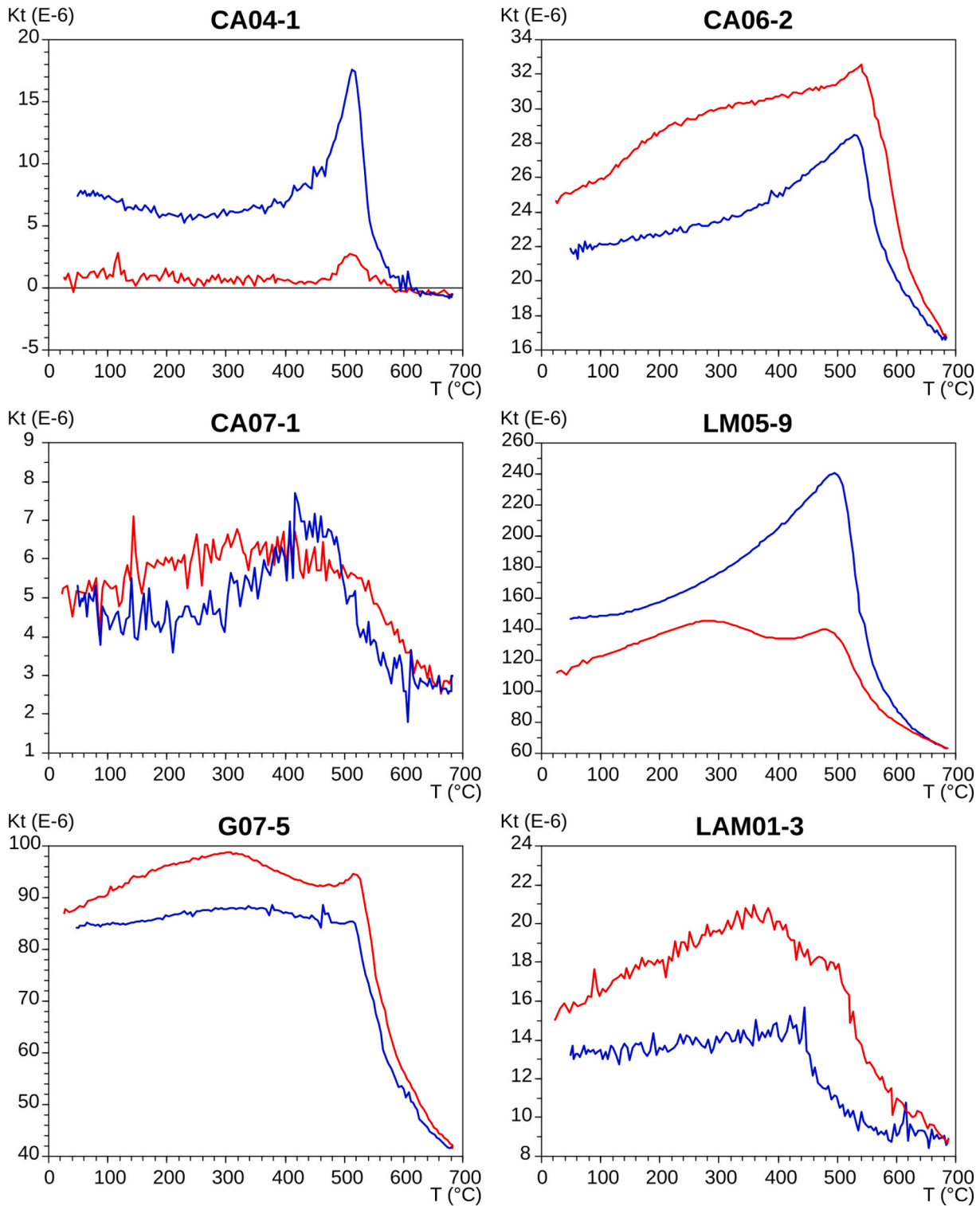


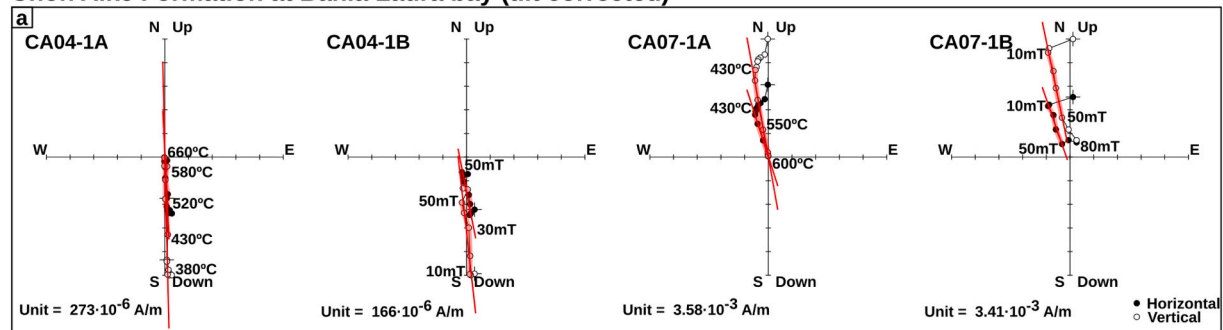
**Fig. 4.** Characteristic thermomagnetic curves (susceptibility vs. T) of the units of the Chon Aike (CA and LM) and La Matilde (G and LAM) formations. Heating curves (red) and cooling curves (blue) indicate that the likely carriers of the ChRM are titanomagnetite and hematite (Dunlop and Özdemir, 1997). (For interpretation of the references to colour in this figure legend, the reader is referred to the web version of this article.)

demagnetization step (bulk susceptibility data is available in Supplementary Data, Table A). The ChRM directions obtained show positive and negative inclinations (Fig. 5b).

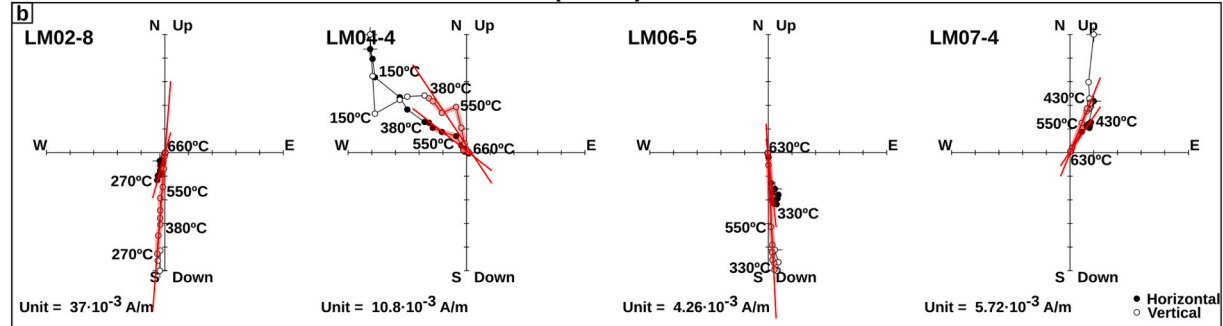
Disperse directions from the LM01 site prevent the calculation of an acceptable mean direction ( $k < 10$ ; Van der Voo, 1990). Therefore, seven mean ChRM directions were calculated by averaging three to nine samples (Table 1). However, the mean ChRM directions from the LM08

and LM10 sites were not considered because their  $\alpha_{95}$  was greater than  $30^\circ$  (Table 1; Fig. 6c). The bedding planes measured in the field were not considered because they were interpreted as rheomorphic structures. Furthermore, after applying the structural correction, the remanence directions dispersed instead of grouping (Fig. 6d), confirming that these are rheomorphic structures related to volcanic flow deformation generated by fissural eruptions (Navarrete, 2021; Navarrete et al., 2020,

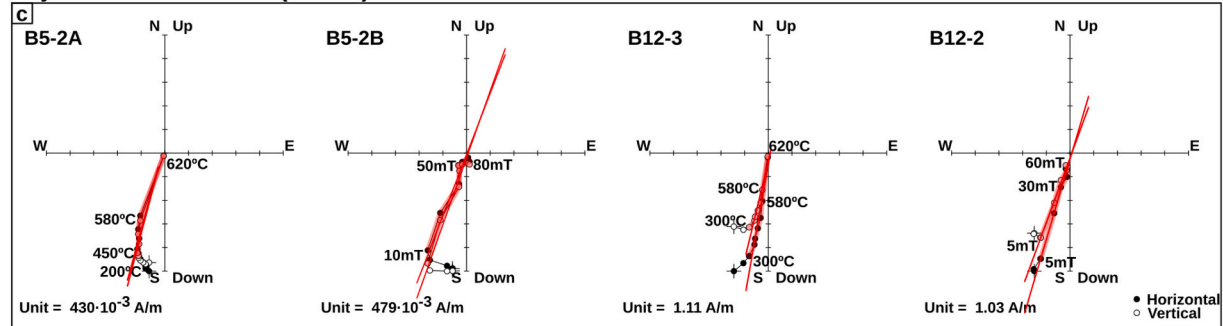
### Chon Aike Formation at Bahía Laura bay (tilt corrected)



### Chon Aike Formation at La Golondrina ranch (in situ)



### Bajo Pobre Formation (in situ)



### La Matilde Formation (tilt corrected)

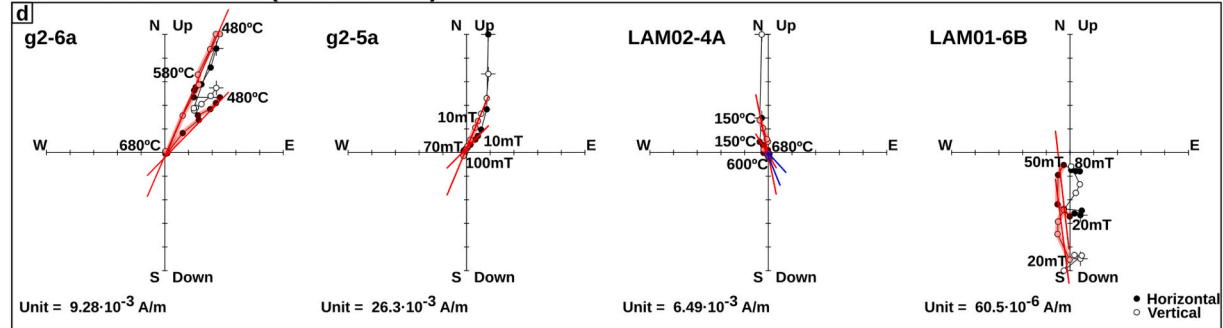
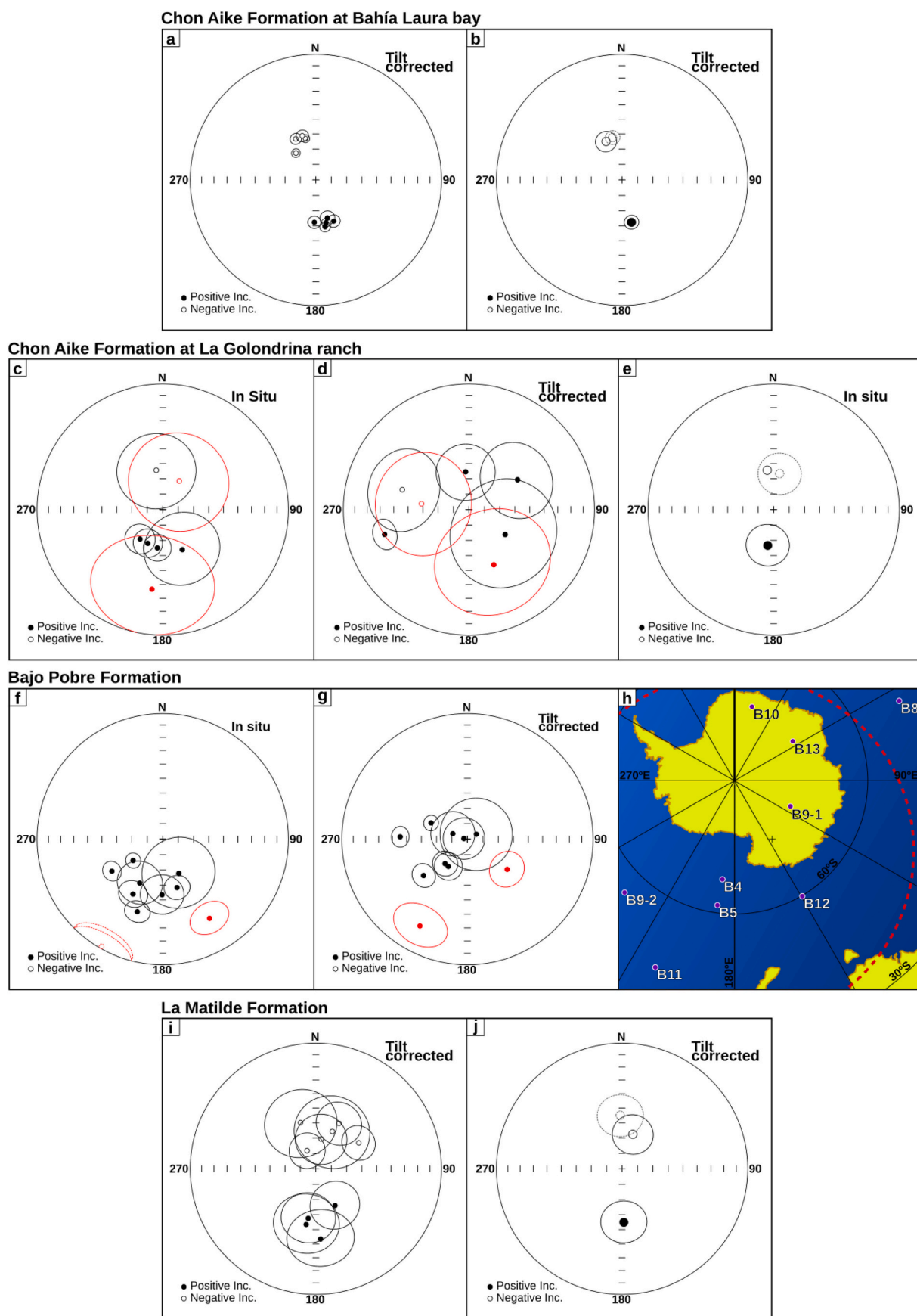


**Fig. 5.** Vector diagrams (Zijderveld, 1967) of representative samples of: (a) Chon Aike Formation from the area near Bahía Laura bay; (b) Chon Aike Formation from the area near the La Golondrina range; (c) Bajo Pobre Formation from the Bosques Petrificados de Jaramillo National Park; (d) La Matilde Formation from the Bosques Petrificados de Jaramillo National Park and the topographic depression of Bajo Grande. The ChRM directions of the A component are highlighted in red and the H component in blue. (For interpretation of the references to colour in this figure legend, the reader is referred to the web version of this article.)

2021). A tilt test was calculated (McFadden, 1990), with a critical  $\xi$  at 95% = 3.44, indicating a negative tilt test at a 95% confidence level (Fig. 6e). Furthermore, a reversal test was calculated with the mean ChRM in situ directions, giving a positive (indeterminate) result with a critical angle of 31.85° and an observed angle of 8.16° (McFadden and McElhinny, 1990). Finally, the VGPs with the in-situ directions for each site (Table 1) and a mean paleomagnetic pole were calculated (Table 2).

#### 4.2. Bajo Pobre Formation

Jovic (2010) performed a geochronological study on units of this formation, presenting an age of  $168.64 \pm 4.34$  Ma obtained by the  $^{40}\text{Ar}$ – $^{39}\text{Ar}$  method (see Fig. 1). From the andesitic rocks of this unit, collected in the Bosques Petrificados de Jaramillo area (Fig. 2c), a ChRM direction was determined between 150 and 200 °C and 600–620 °C, or 5–20 mT and 40–80 mT (Fig. 5c). No relevant changes in the bulk susceptibility of the samples during heating was determined, suggesting



(caption on next page)

**Fig. 6.** Stereographic projection of the paleomagnetic directions of the Chon Aike Formation units near the Bahía Laura Bay: (a) mean ChRM directions, (b) mean values of the normal (negative inclination) and reverse (positive inclination) ChRM mean directions. The Chon Aike Formation units near the La Golondrina ranch: (c) mean in situ ChRM directions (LM08 and LM10 sites are marked with a solid red line), (d) mean tilt-corrected ChRM directions (LM08 and LM10 sites are marked with a solid red line), (e) mean values of the normal (negative inclination) and reverse (positive inclination) ChRM mean directions. The Bajo Pobre Formation units in the eastern area of the Bosques Petrificados de Jaramillo National Park: (f) mean in situ ChRM directions, (g) mean tilt corrected ChRM directions (B6 site is marked with a discontinuous red line, and the B8 site is marked with a solid red line), (h) VGPs plotted on their geographic coordinates (B8 site in outlying position about the 40° cutoff; Wilson et al., 1972). Units of the La Matilde Formation in the eastern area of the Bosques Petrificados de Jaramillo National Park and the topographic depression of Bajo Grande: (i) mean ChRM directions, (j) mean values of the mean ChRM normal (negative inclination) and reverse (positive inclination) ChRM mean directions. The reverse means are transposed to normal polarity (gray-colored discontinuous lined circles) to appreciate the coincidence between the mean values. (For interpretation of the references to colour in this figure legend, the reader is referred to the web version of this article.)

that no secondary magnetic minerals were formed during the heating steps (see Supplementary Data, Table A). The samples from site B2 contain amygdalites filled with calcium carbonate, making them burst above 500 °C when heated in the oven. The ChRM directions present positive inclinations exclusively (Fig. 6f).

With the ChRM directions of three to six samples, the means of the ChRMs per site were calculated. Three sites were not considered since the dispersion of their ChRM was unacceptable ( $k < 10$ ; Van der Voo, 1990). Nine mean ChRM directions were calculated, but site B6 was not considered due to its anomalous direction (Fig. 6f and g). The structural corrections taken in the field were also not considered because, as in the previous case, when applied, the mean directions of the ChRM increased their dispersion (Fig. 6g; Table 1). Thus, a fold test (McFadden, 1990) was calculated, and the result was not statistically significant, although negative. Hence, it was assumed that the remanence was recorded after a non-tectonic structure because the sampled lavas belong to a volcanic dome and their inclinations were acquired during extrusion (see Echeveste et al., 2001). Also, the directions have positive inclinations, opposite to the current geomagnetic field. Therefore, the VGPs per site were calculated using the in-situ directions (Table 1), of which the B8 site was not considered because it was outside the 40° cutoff window (Wilson et al., 1972; Fig. 6h). Thus, a paleomagnetic pole was obtained, with geographic coordinates and statistical parameters (Fisher, 1953) presented in Table 2.

#### 4.3. La Matilde Formation

The La Matilde Formation was sampled in two sites in the Bosques Petrificados de Jaramillo National Park (Fig. 2c) and in 12 sites in the Bajo Grande topographic depression (Fig. 2d), obtaining 92 samples. These rhyolitic tuffs yielded an age of  $157.40 \pm 0.65$  Ma in  $^{40}\text{Ar}$ – $^{39}\text{Ar}$ , as presented above. Several samples burst at around 450 °C in the oven due to the expansion of the biotite crystals because of the alteration into vermiculite (Deer et al., 2013).

A ChRM was determined above 20 mT or between 450 °C and 600–680 °C (A component), except in samples that burst in the oven. Likewise, in some samples, a higher temperature component (H) was determined above 600 °C. The A component was probably carried by titanomagnetite and hematite, and the H component was carried by hematite in some samples (see Fig. 4). ChRMs show positive and negative inclinations (Fig. 5d). During heating, it was possible to detect a substantial increase in susceptibility to 350 °C and then a decrease to 400 °C, probably related to the formation of greigite (see Fig. 4; Dunlop and Özdemir, 1997), after which there were no significant variations in bulk susceptibility of the samples (see Supplementary Data, Table A).

Hence, 11 ChMR mean directions were calculated (Fig. 6i), averaging the results of three to six samples (Table 1). The mean directions of three of the sites were not calculated due to their high dispersion ( $k < 10$ ; Van der Voo, 1990), and two mean directions were not considered because of their unacceptable  $\alpha_{95}$  (Table 1). One of the mean directions corresponds to the H component of the LAM02 site, which was assumed to be the record of a polarity prior to that recorded by the A component. To validate this assumption, a reversal test was calculated with the directions of the A and H components of the LAM02 site (McFadden and McElhinny, 1990), which was class C positive (critical angle = 15.73°;

observed angle = 14.01°). Likewise, a reversal test was calculated with the mean normal and reverse directions, giving a class C positive result (critical angle = 17.9°; observed angle = 14.8°; McFadden and McElhinny, 1990). However, a tilt test yielded a positive but not statistically significant result (McFadden, 1990). Finally, the VGPs per site were obtained with the tilt-corrected directions, and a paleomagnetic pole was calculated with the average of these VGPs (Table 2).

## 5. Discussion

### 5.1. Interpretation of the deformation using paleomagnetic data

Possible tectonic motions within the DM were calculated using the paleomagnetic poles obtained from the units of the Bahía Laura Complex in this work, and those presented by Vilas (1974) and Ruiz González et al. (2019) from the eastern and western outcrops of the Chon Aike Formation, respectively (Fig. 7a). These poles were compared with the mean poles of 180 Ma, 170 Ma, and 160 Ma from the global apparent polar wander paths (APWP) calculated by Kent and Irving (2010), and Torsvik et al. (2012). These mean poles were transferred to South American coordinates, applying the Euler Rotation Parameters taken from each work (Table 3). Possible rotations about the vertical axes of crustal blocks were calculated using the method developed by Demarest (1983), Beck (1980), and Beck et al. (1986).

The rotation about vertical axes of the crustal blocks containing the sampled units decreases from the oldest to the youngest units (Fig. 7b; Table 4). The poles of the Chon Aike Formation in the eastern zone of the DM indicate counterclockwise rotations of  $27^\circ \pm 7^\circ$  in the area near Laura Bay,  $18^\circ \pm 10^\circ$  in the Puerto Deseado area (Vilas, 1974), and  $4^\circ \pm 19^\circ$  that of the La Golondrina ranch area (although this last rotation is not representative since the uncertainty of the method is greater than the result). However, the lower degree of apparent rotation of the units of the La Golondrina ranch area could be ascribed to the fact that these units correspond to the fill of the vertical fissures of the volcanic eruptions, and not to deposits over the rotated blocks (Matthews et al., 2021; Navarrete, 2021; Navarrete et al., 2020, 2021). Furthermore, the pole of the Bajo Pobre Formation in the central area of the DM (see Figs. 2c and 8b) suggests an apparent clockwise rotation of  $19.8^\circ \pm 17.8^\circ$  when compared with the mean poles by Torsvik et al. (2012), which would coincide in the shear direction and the directions of the fault sets described by Giacosa et al. (2010) for the area (see Fig. 2c). However, this rotation is not representative when compared with the mean poles proposed by Kent and Irving (2010) since the uncertainty of the method is greater than the result ( $9.8^\circ \pm 18.4^\circ$ ). Finally, the La Matilde Formation pole and the Chon Aike Formation pole by Ruiz González et al. (2019) indicate that there were no rotations about vertical axes since 157 Ma. The absence of rotations since 119 Ma (Aptian) was also indicated by Somoza et al. (2008) with the obtained pole from the Punta del Barco Formation, part of the Baqueró Group.

Paleomagnetic results partially agree with the proposals of different authors on the evolution of deformation in DM during the Jurassic period. Somoza et al. (2008) propose that there could be a rotation of the entire DM at some point between the Jurassic and the Early Cretaceous. This assumption was based on the results obtained from the Triassic and Cretaceous units of the DM and those from the North Patagonian Massif

**Table 1**

ChRM mean directions, the corresponding VGPs, and the statistical parameters (Fisher, 1953) of the Chon Aike Formation, the Bajo Pobre Formation, and the La Matilde Formation. n / N: number of samples used in the mean calculation vs. total samples per site. <sup>1</sup> Mean directions not considered for having a bigger  $\alpha_{95}$  than 25°.

<sup>2</sup> Mean directions not considered for having an anomalous direction. <sup>3</sup> Mean directions not considered because their respective VGP lies outside the 40° cutoff angle (Wilson et al., 1972).

Site	Site coordinates		n / N	In situ					(Strike / Dip)	Bedding					Tilt corrected					VGP (tilt corrected)	
	Lat. (°S)	Long. (°W)		Dec.	Inc.	R	k	$\alpha_{95}$		Dec.	Inc.	R	k	$\alpha_{95}$	Lat. (°S)	Long. (°E)					
<b>Chon Aike Formation at Bahía Laura bay</b>																					
CA01	48.34041	66.63655	9 / 10	139	69.7	8.95	159	4.1	100 / 12	156.6	60.7	8.95	159	4.1	72.3	36.6					
CA02	48.34108	66.63575	6 / 7	152.4	71.8	5.99	520	2.9	100 / 12	166.6	61.4	5.99	519	2.9	79	50					
CA03	48.34137	66.63792	7 / 8	144.6	74	6.96	163	4.7	100 / 12	163.2	64.1	6.96	163	4.7	78.3	29.2					
CA04	48.34169	66.63557	6 / 6	176.3	74.2	5.98	267	4.1	100 / 12	182	62.4	5.98	267	4.1	85.1	130.9					
CA05	48.33968	66.63280	6 / 6	157.5	69.6	5.99	386	3.4	100 / 12	168.8	58.8	5.99	388	3.4	78.1	66.7					
CA06	48.33410	66.64950	8 / 8	339	-81.8	7.98	381	2.8	44 / 14	323.4	-68.3	7.98	381	2.8	66.5	2					
CA07	48.35312	66.65585	8 / 8	9.6	-72.6	7-98	440	2.6	44 / 14	346	-62.3	7.98	441	2.6	79.2	44.2					
CA08	48.35386	66.65914	7 / 8	348.9	-72.8	6.98	281	3.6	44 / 14	334	-60.2	6.98	283	3.6	70.3	35					
CA09	48.35713	66.65950	8 / 8	2.1	-71	7.96	199	3.9	44 / 14	342.9	-59.9	7.97	201	3.9	75.7	49.1					
Mean normal			4 / 9	357.5	-74.8	3.98	190	6.7		337.4	-62.9	3.98	190	6.7	<b>Paleomagnetic pole</b>						
Mean reverse			5 / 9	153.3	72.3	4.99	280	4.6		167.4	61.7	4.99	281	4.6							
Total mean			9 / 9	343.1	-73.7	8.95	167	4		343	-62.3	8.96	212	3.5	<b>77.3</b>	<b>38</b>					
<b>Chon Aike Formation at La Golondrina ranch</b>																			<b>VGP (in situ)</b>		
LM02	48.15175	67.37790	4 / 8	154	60.9	3.81	15	24.2	292 / 52	58.5	52.6	3.81	15	24.1	70.7	31.7					
LM04	48.14988	67.36859	5 / 9	350.7	-64.1	4.61	10	25.1	340 / 45	286.6	-43.9	4.61	10	25.1	83.3	39.5					
LM05	48.16519	67.38598	10 / 11	217.5	65.8	9.65	26	9.7	289 / 52	355	65.4	8.82	8	18.7	65.2	216.7					
LM06	48.15279	67.37616	7 / 8	188	64.8	6.88	48	8.8	193 / 58	253.5	30.7	6.88	48	8.8	84.4	191.5					
LM07	48.15271	67.37426	5 / 13	203.9	66	4.94	69	9.3	45 / 75	124.7	61.3	4.29	6	35.3	74.1	212.1					
LM08 <sup>1</sup>	48.15237	67.37243	3 / 8	187.7	36.2	2.84	13	36.4	330 / 45	155.8	50.1	2.84	13	36.4	61.3	127.8					
LM10 <sup>1</sup>	48.14985	67.36725	3 / 8	30	-68.6	2.87	15	32.5	340 / 45	276.9	-58.8	2.87	15	32.6	70.5	225.2					
Mean normal			1 / 5	350.7	-64.1	1	0	0		286.6	-43.9	1	0	0							
Mean reverse			4 / 5	189.5	66.4	3.93	46	13.7		13.6	85.9	3.1	3	59.9							
Total mean			5 / 5	5.5	-66.1	4.93	54	10.5		89.3	78.9	3.86	4	48	<b>86</b>	<b>209.8</b>					
<b>Bajo Pobre Formation</b>																			<b>VGP (in situ)</b>		
B4	47.67772	67.95983	3 / 6	207.7	57.6	2.97	76	14.3	279 / 33	290.3	79.9	2.97	76	14.3	67.8	187					
B5	47.67728	67.95983	4 / 5	208.4	48.8	3.97	106	9	290 / 20	215.1	68.4	3.97	106	9	61.8	172.8					
B6 <sup>2</sup>	47.67789	67.96258	4 / 6	209.7	-2	3.92	37	15.4	313 / 25	208.7	22.3	3.92	37	15.4	34.9	149.2					
B8 <sup>3</sup>	47.67858	67.97472	5 / 6	149.4	27.6	4.91	46	11.4	267 / 37	127.3	57.4	4.91	46	11.4	48.4	64.1					
B9-1	47.67822	67.97439	4 / 9	180.7	53.5	3.94	48	13.4	267 / 37	279.6	87.7	3.94	48	13.4	76.3	114.5					
B9-2	47.67822	67.97438	5 / 7	234.2	66.3	4.98	242	4.9	260 / 26	294	64.1	4.98	242	4.9	54.6	224.5					
B10	47.67664	67.97547	4 / 6	154.8	65.4	3.82	16	23.4	260 / 26	61.5	83.4	3.82	16	23.5	73	13.3					
B11	47.67567	67.97694	4 / 6	237.8	50.5	3.99	220	6.2	246 / 30	272	45.5	3.99	220	6.2	43.7	203					
B12	47.67558	67.97750	6 / 6	199.3	38.7	5.94	79	7.6	239 / 32	230.3	52.6	5.94	78	7.6	59.9	149.6					
B13	47.68222	67.98000	5 / 6	163.5	57	4.96	91	8.1	212 / 30	222.4	68.5	4.96	90	8.1	74.3	55.8					
Total mean			8 / 8	199.4	57.7	7.65	20	12.7		253.4	73	7.58	17	14	<b>74.1</b>	<b>181.1</b>					
<b>La Matilde Formation</b>																			<b>VGP (tilt corrected)</b>		
M	47.67632	67.93581	4 / 8	358	-67.8	3.83	18	22.1	30 / 12	341.6	-58.2	3.83	17	22.8	74	48.9					
LAM01	47.66918	67.98501	6 / 6	173	57.3	5.7	17	17	180 / 10	188.7	57.2	5.7	17	16.9	78.3	147.8					
LAM02	47.84225	68.76106	3 / 6	339.3	-62.1	2.98	112	11.7	254 / 15	334.2	-77	2.98	113	11.6	67.9	320.3					
LAM02H	47.84225	68.76106	3 / 6	156.1	48.2	2.97	61	15.9	254 / 15	152.4	63	2.97	62	15.8	70.7	20.9					
LAM03	47.84147	68.76250	4 / 6	359.4	-56.3	3.91	32	16.5	254 / 15	10.1	-70.4	3.91	32	16.5	80.8	251.9					
LAM04 <sup>1</sup>	47.84175	68.75844	3 / 6	206.2	21.8	2.81	11	40	254 / 15	211.7	32.5	2.81	11	40	50.3	162.8					
LAM05	47.84104	68.75762	4 / 6	174	28.5	3.86	22	20.1	254 / 15	176.1	43.3	3.86	22	20.1	67.2	102.1					
G1	47.84058	68.75242	5 / 6	341.2	-75	4.64	11	24.1	148 / 19	23.8	-63.4	4.64	11	24.1	73.4	200					
G2	47.84411	68.76222	5 / 6	59.7	-76.2	4.92	49	11	148 / 19	58.8	-57.2	4.92	49	11	46.8	210.3					
G3	47.84503	68.76578	4 / 6	359.7	-70.6	3.93	42	14.3	148 / 19	27.1	-56.6	3.93	42	14.3	67.5	200.8					
G5	47.84553	68.75778	3 / 5	163	62.3	2.95	38	20.2	148 / 19	189.8	52.9	2.95	38	20.3	73.8	141.9					
G7 <sup>1</sup>	47.83936	68.76458	3 / 6	39.5	-67.8	2.89	19	29.2	254 / 15	80.1	-71.8	2.89	19	29.1	43.1	243.4					
Mean normal			6 / 10	358.2	-69.5	5.9	48	9.7		17.3	-66.5	5.82	27	13							
Mean reverse			4 / 10	167.1	49.4	3.88	26	18.4		178.1	54.9	3.93	43	14.2							
Total mean			10 / 10	352.1	-61.6	9.63	24	10		7.8	-62.2	9.67	27	9.4	<b>84.1</b>	<b>179.2</b>					

by Geuna et al. (2000) and Somoza and Zaffarana (2008). On the other hand, Giacosa et al. (2010) suggested that a change in the directions of the structures was generated by the change of stresses in the DM from the Jurassic extension to the late Early Cretaceous compression. Unifying both criteria, Japas et al. (2013) proposed that the structures had a clockwise rotation about vertical axes from successive increments of progressive deformation and that the vertical-axis rotation of crustal

blocks would have ceased at 156 Ma.

According to the previous references and the results obtained in this work, it could be asserted that the crustal-scale rotations within the DM ceased in the Oxfordian. Also, the kinematic direction of the previous local rotations was not only clockwise but also counterclockwise. In the eastern area of the DM, the paleomagnetic results obtained from the granites of the La Leona Formation of Raethian age (Navarrete et al.,

**Table 2**

Geographic coordinates and statistical parameters (Fisher, 1953) of the calculated paleomagnetic poles. Ar-Ar ages by: a) Féraud et al. (1999), b) this work, c) Matthews et al. (2021), d) Jovic (2010), and e) Ruiz González et al. (2019).

Area	Formation	Age (Ma)	N	Lat (°S)	Long (°E)	K	A95 (°)	References (Fig. 7a)
Puerto Deseado	Chon Aike	177.8 ± 0.4 (a)	22	84	42	20	8	Vilas, 1974 (1)
Bahía Laura	Chon Aike	184.7 ± 0.6 (b)	9	77.3	38	95.3	5.3	This work (2)
La Golondrina	Chon Aike	176.4 ± 5.2 (c)	5	86	209.8	21.4	16.9	This work (3)
Bosques Petrificados	Bajo Pobre	168.6 ± 4.3 (d)	8	74.1	181.1	10.7	17.7	This work (4)
Bajo Grande	La Matilde	157.4 ± 0.7 (b)	10	84.1	179.2	13.6	13.6	This work (5)
W. Ignimbritic Plateau	Chon Aike	155.0 ± 3.5 (e)	23	84.3	191.3	13.3	8.6	Ruiz González et al., 2019 (6)

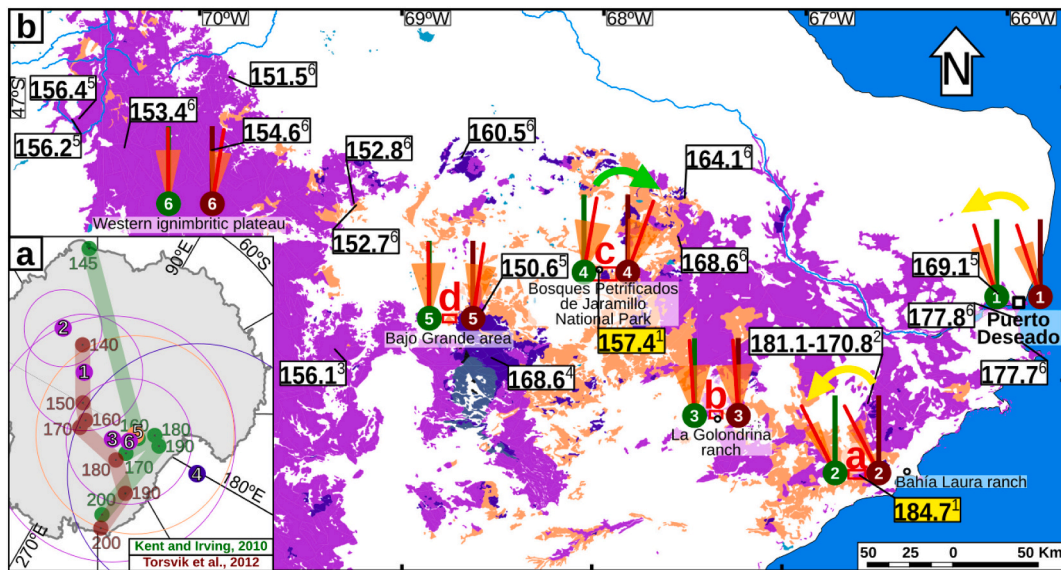


**Fig. 7.** (a) Paleomagnetic poles of the Bahía Laura Complex obtained from some of its formations: 1) Chon Aike in the Puerto Deseado area (Vilas, 1974), 2) Chon Aike in the area near the Bahía Laura bay; 3) Chon Aike in the La Golondrina ranch area; 4) Bajo Pobre in the Bosques Petrificados de Jaramillo National Park; 5) La Matilde in the areas of Bajo Grande and the Bosques Petrificados de Jaramillo National Park; 6) Chon Aike in the western ignimbritic plateau (Ruiz González et al., 2019). Also, the APWP mean poles between 200 Ma and 140 Ma calculated by Kent and Irving (2010), and Torsvik et al. (2012) are presented in green and maroon, respectively. (b) Crustal block rotations about vertical axes shown by the paleomagnetic poles (a) with respect to the global APWP mean poles by Kent and Irving (2010) and the APWP by Torsvik et al. (2012) are presented in green and maroon, respectively. The angle between the vertical and the red line indicates the direction and degree of rotation, taking the vertical line as 0°, and the orange angle shows the degree of uncertainty. Radiometric ages: 1) this work, 2) Matthews et al. (2021), 3) Ruiz González et al. (2019), 4) Jovic (2010), 5) Pankhurst et al. (2000), 6) Féraud et al. (1999). Geochronological method: Ar-Ar is shown in black and U-Pb in green. Geological map modified from Panza et al. (2003). In addition, the sampling areas presented in Fig. 2 are marked with red squares. (For interpretation of the references to colour in this figure legend, the reader is referred to the web version of this article.)

**Table 3**

The 140 Ma to 200 Ma global mean poles calculated by Kent and Irving (2010) and Torsvik et al. (2012) in South American coordinates (applying the Euler Rotation Parameters from each work).

Age (Ma)	N	Lat (°S)	Long (°E)	K	A95 (°)
<u>Kent and Irving (2010)</u>					
200	7	76.2	237.7	253.2	3.8
190	8	80.6	177.7	69.9	6.7
180	8	81.7	170.7	102.9	5.5
170	4	83.4	204.5	200	6.5
160	4	83.6	181.4	152.7	7.5
145	3	67.2	57.0	189.3	9
<u>Torsvik et al. (2012)</u>					
200	39	74.4	238.7	67.9	2.8
190	46	78.5	221.0	53.6	2.9
180	33	83.3	218.9	55	3.4
170	18	86.9	294.3	57.4	4.6
160	19	88.1	304.6	44.3	5.1
150	15	87.4	7.1	36.7	6.4
140	9	80.2	47.4	74.6	6

2019 and references therein) indicate clockwise rotations of the blocks that contain these units (Somoza et al., 2008). However, the units belonging to the Chon Aike Formation east of the DM, of Early Jurassic age (Féraud et al., 1999; Matthews et al., 2021; Navarrete et al., 2020; Pankhurst et al., 2000; this work), indicate counterclockwise rotations (this work). Also, the paleopole presented by Vilas (1974), and considered “cratonic”, in this work indicates a counterclockwise rotation.

On the other hand, in the central part of the DM, the units of the El Tranquilo Group (Fig. 1), from the Middle to Upper Triassic (Jalfin and Herbst, 1995), indicate clockwise rotations (Somoza et al., 2008). Likewise, the Middle Jurassic units of the Bajo Pobre Formation (Jovic, 2010 and references therein), from the Bosques Petrificados de Jaramillo National Park at 60 km NE of the outcrops of El Tranquilo Group (Figs. 1 and 8b), indicate apparent clockwise rotations of a similar magnitude (see Table 4). However, the ~157 Ma La Matilde Formation results from the Bajo Grande area and the Bosques Petrificados de Jaramillo National Park (Figs. 1 and 8b) indicate that these crustal blocks did not register subsequent local vertical rotations of the tectonic blocks. In addition, the paleomagnetic pole of Kimmeridgian age calculated by Ruiz González et al. (2019) of the Chon Aike Formation units from the ignimbritic plateau west of the DM (Fig. 7b) also shows the absence of vertical-axis rotations (~156 Ma). Other paleomagnetic results from this

**Table 4**

Possible tectonic motions calculated with the paleomagnetic poles of the DM compared with the global mean poles calculated by Kent and Irving (2010) and Torsvik et al. (2012). The pole marked with \* corresponds to the calculated by Vilas (1974), and the pole marked with \*\* to the one calculated by Ruiz González et al. (2019).

N	Formation	Mean Age	Kent and Irving, 2010		Torsvik et al., 2012	
			Poleward displacement	Apparent rotation	Poleward displacement	Apparent rotation
1	Chon Aike *	180	$-2.9^\circ \pm 7.1^\circ$	$17.6^\circ \pm 10.0^\circ$	$3.4^\circ \pm 6.4^\circ$	$18.1^\circ \pm 9.2^\circ$
2	Chon Aike "Bahía Laura"	180	$-0.3^\circ \pm 5.6^\circ$	$26.8^\circ \pm 7.7^\circ$	$5.9^\circ \pm 4.6^\circ$	$27.1^\circ \pm 6.6^\circ$
3	Chon Aike "La Golondrina"	180	$-5.6^\circ \pm 13.0^\circ$	$3.7^\circ \pm 19.5^\circ$	$0.7^\circ \pm 12.7^\circ$	$4.0^\circ \pm 19.1^\circ$
4	Bajo Pobre	170	$7.1^\circ \pm 13.8^\circ$	$9.8^\circ \pm 18.4^\circ$	$10.3^\circ \pm 13.4^\circ$	$19.8^\circ \pm 17.8^\circ$
5	La Matilde	160	$-0.2^\circ \pm 11.4^\circ$	$0.8^\circ \pm 16.2^\circ$	$4.1^\circ \pm 10.7^\circ$	$8.4^\circ \pm 15.3^\circ$
6	Chon Aike **	160	$-1.2^\circ \pm 8.4^\circ$	$0.4^\circ \pm 12.0^\circ$	$2.9^\circ \pm 7.3^\circ$	$8.9^\circ \pm 10.8^\circ$

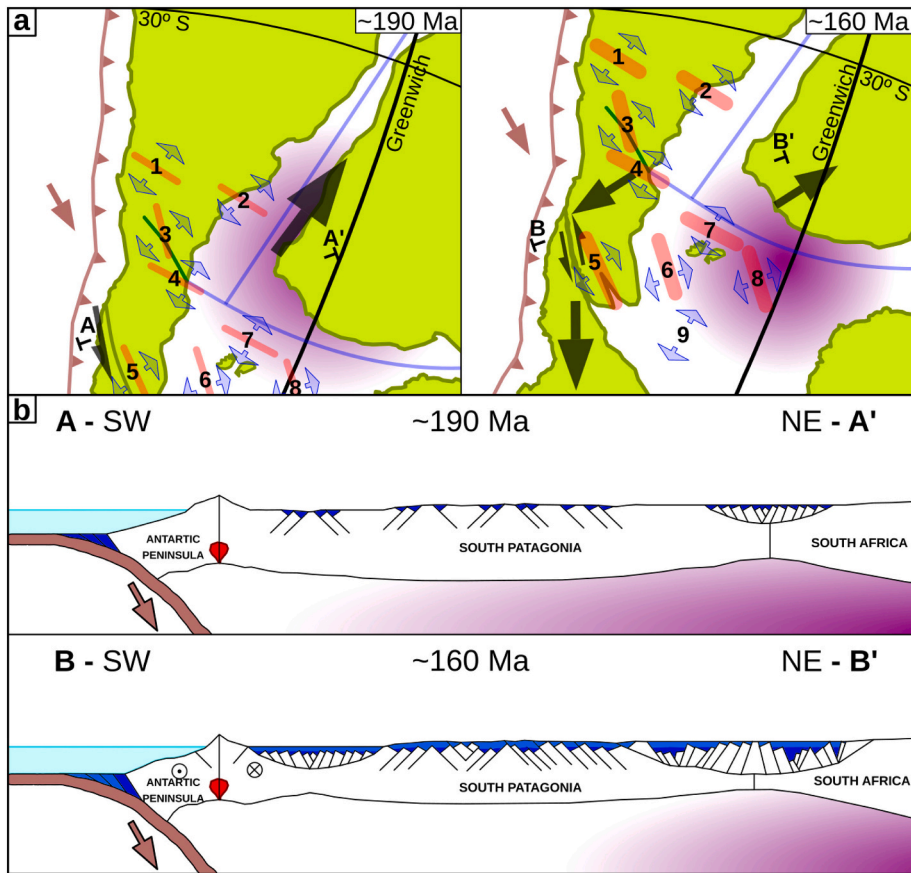


**Fig. 8.** (a) Sketch of the paleogeographic evolution of SW Gondwana. The arrows show the stresses and their relative intensity. The thick red lines mark the beginning of the basins: 1) Neuquén Basin, 2) Colorado Basin, 3) Cañadón Asfalto Basin, 4) San Jorge Gulf Basin, 5) Rocas Verdes Basin, 6) Malvinas Basin, 7) North Malvinas Basin, 8) East Malvinas Basin, and 9) Weddell Sea. Thin blue lines show the posterior arms of the South Atlantic proto-rift. The brown line indicates the trench with an arrow indicating the direction of the subduction of the Phoenix plate. The green line that crosses the central zone of Patagonia corresponds to the potential Paleozoic suture zone described by Renda et al. (2019). (b) Synthetic sections of the tectonic evolution of SW Gondwana from the Late Triassic to the Early Cretaceous (not to scale): Lower Jurassic units are depicted in dark blue and Middle Jurassic units are depicted in blue. The oceanic crust is presented with brown colour and the continental crust with white colour. The purple shading indicates the radiation from the thermal anomaly below SW Gondwana. Based on works by Jordan et al. (2020), van de Lagemaat et al. (2021), Lovecchio et al. (2020) and Riley et al. (2020). (For interpretation of the references to colour in this figure legend, the reader is referred to the web version of this article.)

part of Patagonia, 75 km to the west of the DM, presented by Iglesia Llanos et al. (2003) also show the absence of block rotations about vertical axes since  $\sim 156$  Ma.

Hence, as proposed by Japas et al. (2013), the deformation belts could have simultaneously generated clockwise and anticlockwise vertical-axis rotations of crustal blocks due to the solid anisotropic character of the pre-Jurassic basement reflecting the influence of regional inherited structures (e.g., Navarrete, 2021). Although the different directions of the fault systems are found throughout the DM (Japas et al., 2013; Panza, 1982, 1984; Reimer et al., 1996), the proposed shearing senses do not apply throughout the DM (see Figs. 2a and c).

Thus, due to the generalized NE-SW extension throughout southwestern Gondwana from the Middle Triassic to the Late Jurassic (e.g., Vizán et al., 2017), some rotations of blocks were conditioned by the pre-Jurassic structures from NW-SE to NNO-SSE direction (e.g., Uliana and Biddle, 1988). This extension, triggered by the Tethys slab pull (Vizán et al., 2017), and the high rates of subduction of the Phoenix plate beneath Patagonia plate in a southeastward direction (East et al.,

2020), caused the migration of the Antarctic Peninsula towards the south and the opening of the Rocas Verdes basin (Bastias et al., 2019; Bastias et al., 2021; Cao et al., 2022; Jordan et al., 2020; Suárez et al., 2019; van de Lagemaat et al., 2021), and the beginning of the extension of the later Weddell Sea (Bastias et al., 2021; Jordan et al., 2020; Riley et al., 2020). Finally, the shear component on the extensional stresses which affected Patagonia ceased around 157 Ma, which could be related to the end of the Tethys slab pull (Fig. 8a; Vizán et al., 2017).

For several authors, the overall extensional tectonic regime generated regional crustal thinning of Patagonia (Fig. 8b) and assisted in the generation of anatexitic melts by decompression melting at the base of the continental crust (Echavarria et al., 2005; Foley et al., 2020; Pankhurst and Rapela, 1995; Seitz et al., 2018). This was also assisted by the thermal anomaly located under southwestern Gondwana (Riel et al., 2018), related to the extrusion of fissural volcanism through the multiple normal faults (Navarrete, 2021; Navarrete et al., 2020, 2021). These extensional stresses ended with the opening of the South Atlantic Ocean during the Lower Cretaceous (e.g., Lovecchio et al., 2020).

## 5.2. Paleogeography of South America during the Jurassic Period

To reconstruct the possible drift of the South American continent during the Jurassic period, an APWP was calculated using reliable paleomagnetic poles (Kirschvink, 1980; Van der Voo, 1990). These poles were obtained from units with absolute or relative reliable ages (Bellieni et al., 1992; Féraud et al., 1999; Lossada et al., 2014; Marzoli et al., 1999; Mizusaki et al., 2002; Nomade et al., 2007; Pankhurst et al., 2000; Rapela and Pankhurst, 1993; Renne et al., 1996, 1992; Souza et al., 2003; Stewart et al., 1996; Turner et al., 1994). The moving-age window method was applied to create the APWP (Irving and Irving, 1982), averaging the paleomagnetic poles in 20 Ma windows every 10 Ma (all poles that fall within  $\pm 10$  Ma of the mean age).

The main issue in the calculation of this curve was that many poles could correspond to sites with vertical-axis rotation of crustal blocks or deformations of greater complexity than tilting blocks (e.g., Iglesia Llanos et al., 2006; Rapalini and Lopez de Luchi, 2000; Somoza et al., 2008; Zaffarana and Somoza, 2012). Moreover, other older paleomagnetic poles were not considered because they were calculated without progressive demagnetization, principal component analysis in orthogonal diagrams, or validation tests (e.g., Valencio and Vilas, 1970).

Nevertheless, to calculate the APWP curve from 200 Ma to 140 Ma, only paleomagnetic poles from South American units with ages between 210 Ma and 130 Ma were used (Table 5). The units associated with these poles belong fundamentally to the magmatic provinces of South America that were generated during the Gondwana breakup and the resulting opening of the Atlantic Ocean (Supplementary Data, Table C): the Early Jurassic Central Atlantic Magmatic Province in northeastern Brazil; the Jurassic Chon Aike Igneous Province in Patagonia (Kay et al., 1989); and, the Early Cretaceous Paraná Magmatic Province, which spans in southeastern Brazil, eastern Paraguay, northern Uruguay and Argentina (Cervantes Solano et al., 2015, 2010; Cervantes-Solano et al., 2020; De Min et al., 2003; Ernesto et al., 2003, 1999; Goguitchaichvili et al., 2013; Iglesia Llanos et al., 2003; Mena et al., 2011; Nomade et al., 2000; Raposo and Ernesto, 1995; Ruiz González et al., 2019; Vizán, 1998). Poles obtained from sedimentary units without inclination shallowing issues or crustal block rotations about vertical axes were also included (Kohan Martínez et al., 2019; Vizán et al., 2004).

To make the “absolute” reconstruction of South America between 200 Ma and 140 Ma, the Euler poles of Torsvik et al. (2012) for the Amazonian Craton were used, because none of the poles used in the APWP showed latitudinal or longitudinal differences in the sampling localities with respect to the Amazonian Craton during the Jurassic period. This implies that the Jurassic shape and crustal block configuration of the South American continent were close to the current. In addition, these reconstructions were taken to the West African Craton because this crustal block is assumed to be the one with the least longitudinal displacement during the Jurassic Period (Fig. 9b). This is supported by various authors who have analyzed intraplate displacements between different domains of eastern and southern Africa (e.g., Daly et al., 1989; Jacques, 2003; Lovecchio et al., 2020; Nürnberg and Müller, 1991; Vizán et al., 2017).

Comparing the South American APWP with the global mean poles calculated by Kent and Irving (2010) and Torsvik et al. (2012), in South

American coordinates, shows an overlap from 200 Ma to 180 Ma (Fig. 9a). Furthermore, as can be observed, there is no evidence of a massive true polar wander event called “Jurassic Monster Polar Shift” (Fu et al., 2020; Kent et al., 2015; Kent and Irving, 2010; Muttoni and Kent, 2019). This coincides with other works, where this Jurassic phenomenon is not detected in their paleomagnetic analyses in other terrains of the globe (van Hinsbergen et al., 2019; Kulakov et al., 2021; Mirzaei et al., 2021; Torsvik et al., 2019). Although, there is recognizable a clockwise rotation of South America between 170 Ma and 140 Ma ( $\sim 10^\circ$ ; Fig. 9c).

In addition, the broad uncertainty of the calculated mean of 170 Ma is remarkable (Table 5), caused by the scarce South American poles considered “cratonic” for that time-lapse (see Supplementary Data, Table C). This shortage of Middle Jurassic paleomagnetic poles may be directly related to the tectonic setting during this time lapse, when transpressional deformation was pervasive along southwestern Gondwana, including Patagonia. Moreover, the 170 Ma mean pole is only calculated with two paleomagnetic poles from the same lithostratigraphic unit: the Marifil Complex (Iglesia Llanos et al., 2003; Vizán, 1998).

The 160 Ma mean paleomagnetic pole shows a change in the direction of the path, which coincides with the inferred cessation of the shear component in the extensional stress ( $\sim 157$  Ma). This also is related to the change in the drift direction of the continent, finishing the northward migration around 160 Ma and drifting due to a clockwise rotation until 140 Ma (Fig. 9c).

Additionally, coeval tectonic events probably aided these changes in the tectonic stresses. The Tethys slab pull would have exerted northeastward extensional stresses in the outer parts of Gondwana (Vizán et al., 2017), which coincide with the northward migration of the continent between 200 Ma and 170 Ma (Fig. 9c). Furthermore, this continental migration between 200 Ma and 170 Ma coincides with the back-arc extension in the Weddell Sea rift system proposed by Jordan et al. (2020) and Riley et al. (2020) and the uncoupling of the Antarctic Peninsula (Bastias et al., 2019; Bastias et al., 2021; Suárez et al., 2019; van de Lagemaat et al., 2021). The apparent rotation of the continent (170–160 Ma) may be related to the combination of different tectonic events: 1) the cessation of the northeastward extensional stresses caused in part by Tethys slab-pull (160 Ma; Vizán et al., 2017), 2) the southward migration of the Antarctic Peninsula (Bastias et al., 2019; Bastias et al., 2021; Suárez et al., 2019; van de Lagemaat et al., 2021), 3) the opening of the Rocas Verdes Basin (Calderón et al., 2016; Cao et al., 2022; Müller et al., 2021; Ronda et al., 2019), and 4) the Weddell Sea rifting system (Jordan et al., 2020; Riley et al., 2020). Moreover, these events were controlled by the high rates of subduction of the Phoenix plate (East et al., 2020), which generated the predominance of the extensional stress in the SSW direction (Fig. 9c). The Rocas Verdes basin near the continental margin probably involved asymmetric back-arc spreading by a model of the double-saloon-door rifting and seafloor spreading in a back-arc basin during subduction rollback (e.g., Martin, 2007). The spreading of the Weddell Sea in an N-S direction, which was probably triggered by the southward migration of the Antarctic Peninsula to the south, also aided the overall extension (Bastias et al., 2021). These stresses continued until 140 Ma, when the opening of the South Atlantic Ocean began and the stress interactions changed, starting the closure of the Rocas Verdes Basin (Lovecchio et al., 2020; Müller et al., 2021).

## 6. Conclusions

In this work, four paleomagnetic poles were obtained from the Jurassic Bahía Laura Complex: two from the Chon Aike Formation, located in the eastern part of the DM, one from the Bajo Pobre Formation in the central part of the DM, and the last one from the La Matilde Formation in the central part of the DM. These poles, despite their uncertainties, indicate rotations about vertical axes in clockwise and anticlockwise senses since 185 Ma until 157 Ma. Also, in agreement with

**Table 5**

Geographic coordinates and statistical parameters (Fisher, 1953) of the mean poles calculated from the Jurassic South American APWP.

Mean poles ages	N	Lat (°S)	Long (°E)	K	A95 (°)
140	11	-86.1	73.8	578.5	1.9
150	5	-85.3	154.0	163.6	6
160	4	-84.0	179.3	1159	2.7
170	2	-83.0	176.3	156.5	20.1
180	3	-82.1	198.1	138.9	10.5
190	4	-80.1	217.7	879.4	3.1
200	4	-80.4	243.1	178.3	6.9

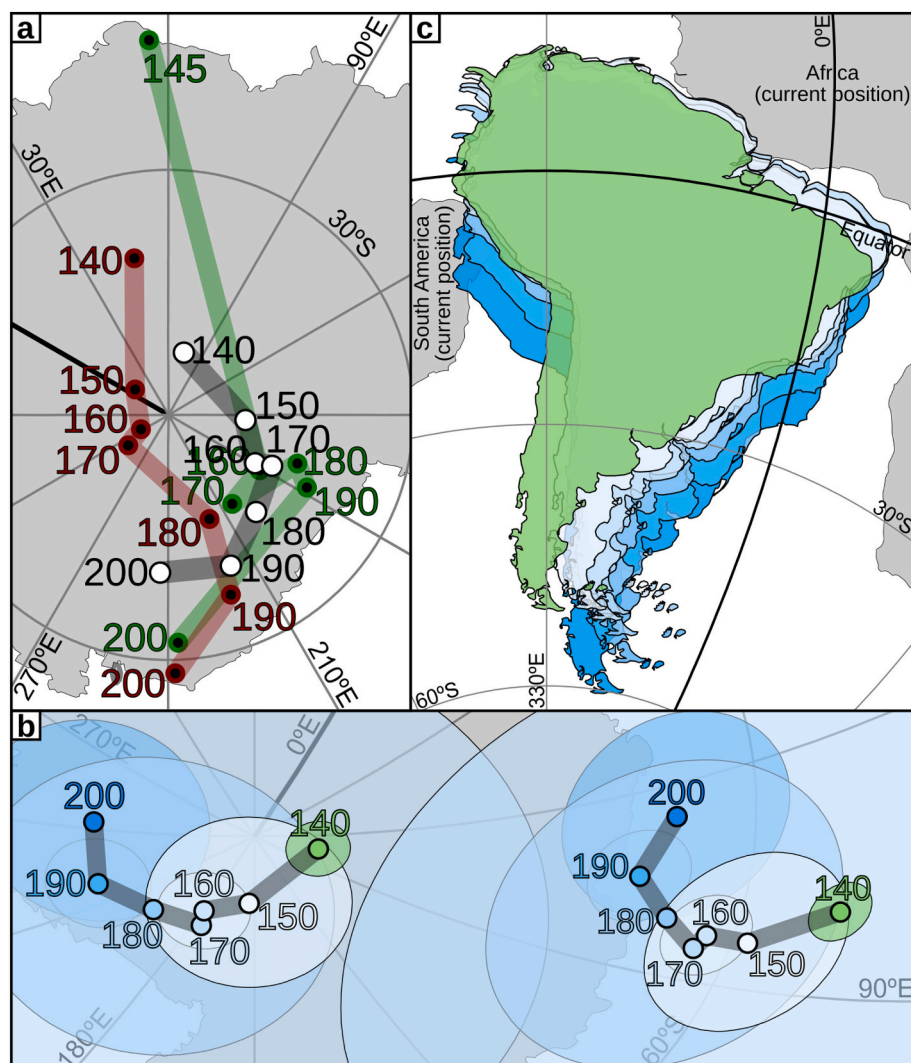


**Fig. 9.** (a) Comparison of the calculated APWP (white circles) and those presented by Kent and Irving (2010) in green and Torsvik et al. (2012) in maroon (in South American coordinates). (b) Calculated South American APWP between 200 Ma and 140 Ma in South American (left) and NW African coordinates (right). (c) The apparent drift of South America between 200 Ma and 140 Ma. (For interpretation of the references to colour in this figure legend, the reader is referred to the web version of this article.)

other authors, the younger pole indicates no vertical-axis rotations of crustal blocks since 157 Ma.

Finally, a Jurassic APWP for South America was calculated to analyze the paleogeography and the continental drift during Jurassic times. The APWP shows a coincidence with the tectonic history of the DM and indicates the possible causes of the change in stresses at around 160 Ma from transtensional to purely extensional. This change could be triggered by the combination of several events, which include the cessation of the northeastward extension with the end of the Tethys slab pull, and the southward migration of the Antarctic Peninsula, generating the space for the opening and extension of the Rocas Verdes Basin and the Weddell Sea. Also, the APWP does not show evidence of a massive Jurassic true polar wander event. In addition, an apparent clockwise rotation of the continent ( $\sim 10^\circ$ ) from 160 Ma to 140 Ma can be explained by the tectonics of the SW Gondwana at that time.

#### CRediT authorship contribution statement

**V. Ruiz González:** Conceptualization, Formal analysis, Investigation, Writing – original draft. **E.M. Renda:** Investigation, Writing – review & editing. **H. Vizán:** Investigation, Validation, Supervision, Funding acquisition, Writing – review & editing. **M. Ganerød:** Formal analysis, Investigation. **C.G. Puigdomenech:** Writing – review & editing. **C.B. Zaffarana:** Supervision, Writing – review & editing.

#### Declaration of Competing Interest

The authors declare that they have no known competing financial interests or personal relationships that could have appeared to influence the work reported in this paper.

#### Acknowledgments

We thank Dr. Graeme K. Taylor for his help in the field and his constructive suggestions, and Dr. Rubén Somoza for his fieldwork and for being the intellectual author of this work. We also thank CONICET (Consejo Nacional de Investigaciones Científicas de Argentina) and UBA (Universidad de Buenos Aires) for the financial support (PIP 11220120100200CO and UBACyT 20020150100069BA, respectively).

#### Appendix A. Supplementary data

Supplementary data to this article can be found online at <https://doi.org/10.1016/j.tecto.2022.229389>.

#### References

- Alric, V.I., Haller, M.J., Féraud, G., Bertrand, H., Zubia, M., 1996. Cronología 40 Ar/ 39 Ar del volcanismo jurásico de la Patagonia extrandina. In: Actas. Presented at the XIII Congreso Geológico Argentino y III Congreso de Exploración de Hidrocarburos, Asociación Geológica Argentina, Buenos Aires, pp. 243–250.

- Archangelsky, S., 1967. Estudio de la Formación Baqueró. Cretácico Inferior de Santa Cruz, Argentina. *Revista del Museo de La Plata* 5, 63–171.
- Arrondo, O.G., 1972. Estudio geológico y paleontológico en la zona de la estancia La Juanita y alrededores, provincia de Santa Cruz, Argentina. *Revista del Museo de La Plata* 7, 1–194.
- Bastias, J.M., Israel, L., Hervé, F., Spikings, R., Pankhurst, R., Castillo, P., Fanning, M., Ugalde, R., 2019. The Byers Basin: Jurassic-cretaceous tectonic and depositional evolution of the forearc deposits of the South Shetland Islands and its implications for the northern Antarctic Peninsula. *Int. Geol. Rev.* 0, 1–18. <https://doi.org/10.1080/00206814.2019.1655669>.
- Bastias, J., Spikings, R., Riley, T., Ulianov, A., Grunow, A., Chiaradia, M., Hervé, F., 2021. A revised interpretation of the Chon Aike magmatic province: active margin origin and implications for the opening of the Weddell Sea. *Lithos* 386–387, 106013. <https://doi.org/10.1016/j.lithos.2021.106013>.
- Beck, M.E., 1980. Paleomagnetic record of plate-margin tectonic processes along the western edge of North America. *J. Geophys. Res. Solid Earth* 85, 7115–7131. <https://doi.org/10.1029/JB085iB12p07115>.
- Beck, M.E., Burmester, R.F., Craig, D.E., Gromme, C.S., Wells, R.E., 1986. Paleomagnetism of Middle Tertiary volcanic rocks from the Western Cascade Series, northern California. *J. Geophys. Res. Solid Earth* 91, 8219–8230. <https://doi.org/10.1029/JB091iB08p08219>.
- Bellieni, G., Macedo, M.H.F., Petrini, R., Piccirillo, E.M., Cavazzini, G., Comin-Chiaromonti, P., Ernesto, M., Mamedo, J.W.P., Martins, G., Melfi, A.J., Pacca, I.G., De Min, A., 1992. Evidence of magmatic activity related to Middle Jurassic and lower cretaceous rifting from northeastern Brazil (Ceará-Mirim): K/Ar age, palaeomagnetism, petrology and Sr/18Nd isotope characteristics. *Chem. Geol.* 97, 9–32. [https://doi.org/10.1016/0009-2541\(92\)90133-P](https://doi.org/10.1016/0009-2541(92)90133-P).
- Bilmes, A., D'Elia, L., Franzese, J.R., Veiga, G.D., Hernández, M., 2013. Miocene block uplift and basin formation in the Patagonian foreland: the Gastre Basin, Argentina. *Tectonophysics* 601, 98–111. <https://doi.org/10.1016/j.tecto.2013.05.001>.
- Butler, R.F., 1992. *Paleomagnetism: Magnetic Domains to Geologic Terranes*. Blackwell Scientific Publications.
- Calderón, M., Fildani, A., Hervé, F., Fanning, C.M., Weislogel, A., Cordani, U., 2007. Late Jurassic bimodal magmatism in the northern sea-floor remnant of the Rocas Verdes basin, southern Patagonian Andes. *J. Geol. Soc.* 164, 1011–1022. <https://doi.org/10.1144/0016-76492006-102>.
- Calderón, M., Hervé, F., Fuentes, F., Fosdick, J.C., Sepúlveda, F., Galaz, G., 2016. Tectonic evolution of paleozoic and mesozoic andean metamorphic complexes and the Rocas Verdes Ophiolites in Southern Patagonia. In: Ghiglione, M. (Ed.), *Geodynamic Evolution of the Southernmost Andes: Connections with the Scotia Arc*, Springer Earth System Sciences. Springer International Publishing, Cham, pp. 7–36. [https://doi.org/10.1007/978-3-319-39727-6\\_2](https://doi.org/10.1007/978-3-319-39727-6_2).
- Cao, S.J., Torres Carbonell, P.J., Bordese, S., Lovecchio, J.P., 2022. Early rifting during marginal basin development: petrography, microstructure, and detrital zircon U-Pb geochronology of the Lapataia Formation, Argentine Fuegian Andes. *Basin Res.* 00, 1–21. <https://doi.org/10.1111/bre.12664>.
- Cervantes Solano, M., Goguitchaichvili, A., Sánchez Bettucci, L., Cejudo Ruiz, R., Calvo-Rathert, M., Ruiz-Martínez, V.C., Soto, R., Alva-Valdivia, L.M., 2010. Paleomagnetism of early cretaceous areappy formation (Northern Uruguay). *Stud. Geophys. Geod.* 54, 533–546. <https://doi.org/10.1007/s11200-010-0032-8>.
- Cervantes Solano, M., Goguitchaichvili, A., Mena, M., Alva-Valdivia, L., Contreras, J.M., Ruiz, R.C., Loera, H.L., Soler, A.M., Urrutia-Fucugauchi, J., 2015. Paleomagnetic pole positions and geomagnetic secular variation from the Cretaceous Ponta Grossa Dike Swarm (Brazil). *Geofis. Int.* 54, 167–178. <https://doi.org/10.1016/j.gi.2015.04.012>.
- Cervantes-Solano, M., Goguitchaichvili, A., Sánchez Bettucci, L., Morales-Contreras, J., Gogorza, C., Núñez, P., 2020. An integrated paleomagnetic and multispecimen paleointensity study from the late Jurassic Zapicán dike swarm (Uruguay). *J. S. Am. Earth Sci.* 104, 102815. <https://doi.org/10.1016/j.jsames.2020.102815>.
- Cladera, G., Andreis, R., Archangelsky, S., Cúneo, R., 2002. Estratigrafía del Grupo Baqueró, Patagonia (provincia de Santa Cruz, Argentina). *Ameghiniana* 39, 3–20.
- Cobos, J.C., Panza, J.L.A., Zubía, M.A., Figari, E.G., Cardinali, G., Lucero, M., Borderas, M., 2003. Hoja Geológica 4769-I El Pluma. Servicio Geológico Minero Argentino. Instituto de Geología y Recursos Minerales.
- Creer, K.M., Mitchell, J.G., Abou Deeb, J., 1972. Palaeomagnetism and radiometric age of the Jurassic Chon Aike formation from Santa Cruz Province, Argentina: implications for the opening of the South Atlantic. *Earth Planet. Sci. Lett.* 14, 131–138. [https://doi.org/10.1016/0012-821X\(72\)90092-1](https://doi.org/10.1016/0012-821X(72)90092-1).
- Daly, M.C., Chorowicz, J., Fairhead, J.D., 1989. Rift basin evolution in Africa: the influence of reactivated steep basement shear zones. *Geol. Soc. Spec. Publ.* 44, 309–334. <https://doi.org/10.1144/GSL.SP.1989.044.01.17>.
- Dalziel, I.W.D., de Wit, M.J., Palmer, K.F., 1974. Fossil marginal basin in the southern Andes. *Nature* 250, 291–294. <https://doi.org/10.1038/250291a0>.
- Dalziel, I.W.D., Lawver, L.A., Murphy, J.B., 2000. Plumes, orogenesis, and supercontinental fragmentation. *Earth Planet. Sci. Lett.* 178, 1–11. [https://doi.org/10.1016/S0012-821X\(00\)00061-3](https://doi.org/10.1016/S0012-821X(00)00061-3).
- De Giusto, J.M., Di Persia, S.A., Pezzi, E., 1980. Nesocratón del Deseado. In: *2º Simposio de Geología Regional Argentina. Academia Nacional de Ciencias, Córdoba*, pp. 1389–1430.
- De Min, A., Piccirillo, E.M., Marzoli, A., Bellieni, G., Renne, P.R., Ernesto, M., Marques, L.S., 2003. The Central Atlantic Magmatic Province (CAMP) in Brazil: petrology, geochemistry, 40Ar/39Ar ages, paleomagnetism and geodynamic implications. In: *The Central Atlantic Magmatic Province: Insights from Fragments of Pangea*. American Geophysical Union (AGU), pp. 91–128. <https://doi.org/10.1029/136GM06>.
- Deer, W.A., Howie, R.A., Zussman, J., 2013. *An Introduction to the Rock-Forming Minerals*, 3rd ed. Mineralogical Society of Great Britain and Ireland, London.
- Demarest, H.H., 1983. Error analysis for the determination of tectonic rotation from paleomagnetic data. *J. Geophys. Res. Solid Earth* 88, 4321–4328. <https://doi.org/10.1029/JB088iB05p04321>.
- Di Persia, C., 1955. Informe previo al Levantamiento Geológico en escala 1:100.000 de la zona Norte del Territorio de Santa Cruz, al sur del río Deseado. In: *Segunda Campaña (Inédito). Yacimientos Petrolíferos Fiscales, Buenos Aires*.
- Di Persia, C., 1958. Informe previo al Levantamiento Geológico en escala 1:100.000 de la zona Norte del Territorio de Santa Cruz, al sur del río Deseado. In: *Quinta Campaña (Inédito). Yacimientos Petrolíferos Fiscales, Buenos Aires*.
- Di Persia, C., 1962. Acerca del descubrimiento del Precámbrico en la Patagonia Extrandina (provincia de Santa Cruz). In: *Actas. Presented at the Primeras Jornadas Geológicas Argentinas, San Juan*, pp. 65–68.
- Dunlop, D.J., Özdemir, Ö., 1997. *Rock Magnetism: Fundamentals and Frontiers*, Cambridge Studies in Magnetism. Cambridge University Press, Cambridge. <https://doi.org/10.1017/CBO9780511612794>.
- Eagles, G., 2007. New angles on South Atlantic opening. *Geophys. J. Int.* 168, 353–361. <https://doi.org/10.1111/j.1365-246X.2006.03206.x>.
- East, M., Müller, R.D., Williams, S., Zahirovic, S., Heine, C., 2020. Subduction history reveals cretaceous slab superflux as a possible cause for the mid-cretaceous plume pulse and superswell events. *Gondwana Res.* 79, 125–139. <https://doi.org/10.1016/j.gr.2019.09.001>.
- Echavarría, L.E., 1999. Evolución geológica y su relación con la mineralización epitermal en el área El Dorado-Monserrat, Macizo del Deseado, Santa Cruz, Argentina. *Studia Geol. Salmanticensis* 35, 21–39.
- Echavarría, L.E., Schalamuk, I.B., Etcheverry, R.O., 2005. Geologic and tectonic setting of Deseado Massif epithermal deposits, Argentina, based on El Dorado-Monserrat. *J. S. Am. Earth Sci.* 19, 415–432. <https://doi.org/10.1016/j.jsames.2005.06.005>.
- Echeveste, H., Fernández, R.R., Bellieni, G., Tessone, M.O.R., Llambias, E.J., Schalamuk, I.B.A., Piccirillo, E.M., Min, A.D., 2001. Relaciones entre las Formaciones Bajo Pobre y Chon Aike [Jurásico Medio a Superior] en el área Estancia El Félix-Cerro Huemul, zona centro-occidental del Macizo del Deseado, provincia de Santa Cruz. *Rev. Asoc. Geol. Argent.* p. 56.
- Ernesto, M., Raposo, M.I.B., Marques, L.S., Renne, P.R., Diogo, L.A., de Min, A., 1999. Paleomagnetism, geochemistry and 40Ar/39Ar dating of the North-eastern Paraná Magmatic Province: tectonic implications. *J. Geodyn.* 28, 321–340. [https://doi.org/10.1016/S0264-3707\(99\)00013-7](https://doi.org/10.1016/S0264-3707(99)00013-7).
- Ernesto, M., Bellieni, G., Piccirillo, E.M., Marques, L.S., de Min, A., Pacca, I.G., Martins, G., Mamedo, J.W.P., 2003. Paleomagnetic and geochemical constraints on the timing and duration of the CAMP activity in Northeastern Brazil. In: *The Central Atlantic Magmatic Province: Insights from Fragments of Pangea*. American Geophysical Union (AGU), pp. 129–149. <https://doi.org/10.1029/136GM07>.
- Escosteguy, L.D., Dal Molin, C.N., Franchi, M., Geuna, S.E., Lapiro, O.R., 2003. Hoja Geológica 4772-II Lago Buenos Aires. Servicio Geológico Minero Argentino. Instituto de Geología y Recursos Minerales.
- Féraud, G., Alric, V., Fornari, M., Bertrand, H., Haller, M., 1999. 40Ar/39Ar dating of the Jurassic volcanic province of Patagonia: migrating magmatism related to Gondwana break-up and subduction. *Earth Planet. Sci. Lett.* 172, 83–96. [https://doi.org/10.1016/S0012-821X\(99\)00190-9](https://doi.org/10.1016/S0012-821X(99)00190-9).
- Fernández, R.R., Tessone, M.O.R., Echeveste, H.J., Moreira, P., Carlini, M., 2016. Geología y mineralización del área “Estancia San Pedro”, Macizo del Deseado, Provincia de Santa Cruz. *Rev. Asoc. Geol. Argent.* 73, 388–404.
- Ferpozzi, F.J., Johanis, P.E., 2004. Bloque Santa Cruz 1968. Digitalización, Reprocesamiento y Edición. Contribuciones Técnicas, Levantamiento Aeromagnético Analógico, pp. 1–16.
- Ferris, J.K., Vaughan, A.P.M., Storey, B.C., 2000. Relics of a complex triple junction in the Weddell Sea embayment, Antarctica. *Earth Planet. Sci. Lett.* 178, 215–230. [https://doi.org/10.1016/S0012-821X\(00\)0076-5](https://doi.org/10.1016/S0012-821X(00)0076-5).
- Feruglio, E., 1946. Sistemas orográficos de la Argentina. In: *Geografía de La República Argentina. Sociedad Argentina de Estudios Geográficos*, pp. 1–536.
- Feruglio, E., 1949. Descripción geológica de la Patagonia. Dirección Nacional de Yacimientos Petrolíferos Fiscales, Buenos Aires.
- Fisher, R.A., 1953. Dispersion on a sphere. *Proc. R. Soc. Lond. A* 217, 295–305. <https://doi.org/10.1098/rspa.1953.0064>.
- Foley, M., Putlitz, B., Baumgartner, L., Guillermín, Z., Bégué, F., 2020. Magmas of the El Quemado Complex (Chon Aike Silicic Igneous Province, Patagonia): Elevated Oxygen Isotope Signatures Across Space and Time. *EGU General Assembly 2020*, Online, 4–8 May 2020, EGU2020-21265. <https://doi.org/10.5194/egusphere-egu2020-21265>.
- Fraccia, D., Giacosa, R., 2006. Evolución estructural del basamento ígneo-metamórfico en la estancia Las Tres Hermanas, noreste de la comarca del Deseado, Santa Cruz. *Rev. Asoc. Geol. Argent.* 61, 118–131.
- Fu, R.R., Kent, D.V., Hemming, S.R., Gutiérrez, P., Creveling, J.R., 2020. Testing the occurrence of late Jurassic true polar wander using the La Negra volcanics of northern Chile. *Earth Planet. Sci. Lett.* 529, 115835. <https://doi.org/10.1016/j.epsl.2019.115835>.
- Geuna, S.E., Somoza, R., Vizán, H., Figari, E.G., Rinaldi, C.A., 2000. Paleomagnetism of Jurassic and Cretaceous rocks in Central Patagonia: a key to constrain the timing of rotations during the breakup of southwestern Gondwana? *Earth Planet. Sci. Lett.* 181, 145–160. [https://doi.org/10.1016/S0012-821X\(00\)00198-9](https://doi.org/10.1016/S0012-821X(00)00198-9).
- Ghidella, M.E., Yáñez, G., LaBrecque, J.L., 2002. Revised tectonic implications for the magnetic anomalies of the western Weddell Sea. *Tectonophysics. Mag. Anomalies Antarctic* 347, 65–86. [https://doi.org/10.1016/S0040-1951\(01\)00238-4](https://doi.org/10.1016/S0040-1951(01)00238-4).

- Giacosa, R.E., Franchi, M., Genini, A., Panza, J.L.A., 2001. Hojas Geológicas 4772-III Lago Belgrano y 4772-IV Lago Posadas. Servicio Geológico Minero Argentino. Instituto de Geología y Recursos Minerales.
- Giacosa, R.E., Genini, A., 1998. Hoja Geológica 4766-III/IV Puerto Deseado. Servicio Geológico Minero Argentino, Instituto de Geología y Recursos Minerales.
- Giacosa, R.E., Márquez, M.M., Panza, J., 2002. BASAMENTO PALEOZOICO INFERIOR DEL MACIZO DEL DESEADO. In: Geología y Recursos Naturales de Santa Cruz. XV Congreso Geológico Argentino. El Calafate, pp. 1–11.
- Giacosa, R., Zubia, M., Sánchez, M., Allard, J., 2010. Meso-Cenozoic tectonics of the southern Patagonian foreland: Structural evolution and implications for Au–Ag veins in the eastern Deseado Region (Santa Cruz, Argentina). *J. S. Am. Earth Sci.* 30, 134–150. <https://doi.org/10.1016/j.jsames.2010.09.002>.
- Goguitchaichvili, A., Solano, M.C., Camps, P., Bettucci, L.S., Mena, M., Trindade, R., Reyes, B.A., Morales, J., Loera, H.L., 2013. The Earth's magnetic field prior to the cretaceous Normal Superchron: new palaeomagnetic results from the Alto Paraguay Formation. *Int. Geol. Rev.* 55, 692–704. <https://doi.org/10.1080/00206814.2012.732801>.
- Grunow, A.M., 1993. Creation and destruction of Weddell Sea floor in the Jurassic. *Geology* 21, 647–650. [https://doi.org/10.1130/0091-7613\(1993\)021<0647:CADS>2.3.CO;2](https://doi.org/10.1130/0091-7613(1993)021<0647:CADS>2.3.CO;2).
- Grunow, A.M., Kent, D.V., Dalziel, I.W.D., 1987. Mesozoic evolution of West Antarctica and the Weddell Sea Basin: new paleomagnetic constraints. *Earth Planet. Sci. Lett.* 86, 16–26. [https://doi.org/10.1016/0012-821X\(87\)90184-1](https://doi.org/10.1016/0012-821X(87)90184-1).
- Guido, D.M., 2004. Subdivisión litofacial e interpretación del volcanismo jurásico (Grupo Bahía Laura) en el este del Macizo del Deseado, provincia de Santa Cruz. *Rev. Asoc. Geol. Argent.* 59, 727–742.
- Guido, D., Escayola, M., de Barrio, R., Schalamuk, I., Takashi Onoe, A., 2004. Edad y rasgos petrográficos y geoquímicos de cuerpos subvolcánicos asignables a la Formación Cerro León, este del Macizo del Deseado, Santa Cruz. *Rev. Asoc. Geol. Argent.* 59, 707–714.
- Guido, D., Escayola, M., de Barrio, R., Schalamuk, I., Franz, G., 2006. La Formación Bajo Pobre (Jurásico) en el este del Macizo del Deseado, Patagonia: vinculación con el Grupo Bahía Laura. *Rev. Asoc. Geol. Argent.* 61, 187–196.
- Harrington, H.J., 1962. Paleogeographic Development of South America. *AAPG Bull.* 46, 1773–1814. <https://doi.org/10.1306/BC7438F1-16BE-11D7-8645000102C1865D>.
- Herbst, R., 1965. La flora fósil de la Formación Roca Blanca, provincia de Santa Cruz, Patagonia, con consideraciones geológicas y estratigráficas., *Opera Lilloana*. ed. Tucumán.
- Hole, M.J., Ellam, R.M., Macdonald, D.I.M., Kelley, S.P., 2016. Gondwana break-up related magmatism in the Falkland Islands. *J. Geol. Soc.* 173, 108–126. <https://doi.org/10.1144/jgs2015-027>.
- Homovc, J.F., Constantini, L., 2001. Hydrocarbon exploration potential within intraplate shear-related depocenters: Deseado and San Julian Basins, Southern Argentina. *AAPG Bull.* 85, 1795–1816. <https://doi.org/10.1306/8626D077-173B-11D7-8645000102C1865D>.
- Huang, C., Zhang, N., Li, Z.-X., Ding, M., Dang, Z., Pourteau, A., Zhong, S., 2019. Modeling the inception of supercontinent breakup: stress state and the importance of orogens. *Geochem. Geophys. Geosyst.* 20, 4830–4848. <https://doi.org/10.1029/2019GC008538>.
- Iglesia Llanos, M.P., Lanza, R., Riccardi, A.C., Geuna, S., Laurenzi, M.A., Ruffini, R., 2003. Palaeomagnetic study of the El Quemado complex and Marifil formation, Patagonian Jurassic igneous province, Argentina. *Geophys. J. Int.* 154, 599–617. <https://doi.org/10.1046/j.1365-246X.2003.01923.x>.
- Iglesia Llanos, M.P., Riccardi, A.C., Singer, S.E., 2006. Palaeomagnetic study of Lower Jurassic marine strata from the Neuquén Basin, Argentina: a new Jurassic apparent polar wander path for South America. *Earth Planet. Sci. Lett.* 252, 379–397. <https://doi.org/10.1016/j.epsl.2006.10.006>.
- Irving, E., Irving, G.A., 1982. Apparent polar wander paths carboniferous through cenozoic and the assembly of Gondwana. *Geophys. Surv.* 5, 141–188. <https://doi.org/10.1007/BF01453983>.
- Jacques, J.M., 2003. A tectonostratigraphic synthesis of the Sub-Andean basins: inferences on the position of south American intraplate accommodation zones and their control on South Atlantic opening. *J. Geol. Soc.* 160, 703–717. <https://doi.org/10.1144/0016-764902-089>.
- Jalfin, G.A., Herbst, R., 1995. La flora triásica del Grupo El Tranquilo, Provincia de Santa Cruz (Patagonia). *Estratigrafía. Ameghiniana* 32, 221–229.
- Japas, M.S., 2001. Modelo cinematográfico neopaleozoico para el sector nororiental del Macizo Norpatagónico, Argentina. *J. Iber. Geol.* 91–121 <https://doi.org/10.5209/JIGE.34004>.
- Japas, M.S., Sruoga, P., Kleiman, L.E., Gayone, M.R., Maloberti, A., Comito, O., 2013. Cinematografía de la extensión jurásica vinculada a la Provincia Silícea Chon Aike, Santa Cruz, Argentina. *Rev. Asoc. Geol. Argent.* 70, 16–30.
- Jordan, T.A., Ferraccioli, F., Leat, P.T., 2017. New geophysical compilations link crustal block motion to Jurassic extension and strike-slip faulting in the Weddell Sea Rift System of West Antarctica. *Gondwana Res.* 42, 29–48. <https://doi.org/10.1016/j.gr.2016.09.009>.
- Jordan, T.A., Riley, T.R., Siddoway, C.S., 2020. The geological history and evolution of West Antarctica. *Nat. Rev. Earth Environ.* 1, 117–133. <https://doi.org/10.1038/s43017-019-0013-6>.
- Jovic, S.M., 2010. Geología y metalogénesis de las mineralizaciones polimetálicas del área El Tranquilo (Cerro León), sector central del Macizo del Deseado, provincia de Santa Cruz. Editorial de la Universidad Nacional de La Plata (EDULP), La Plata.
- Kay, S.M., Ramos, V.A., Mpodozis, C., Sruoga, P., 1989. Late Paleozoic to Jurassic silicic magmatism at the Gondwana margin: Analogy to the Middle Proterozoic in North America? *Geology* 17, 324–328. [https://doi.org/10.1130/0091-7613\(1989\)017<0324:LPTJSM>2.3.CO;2](https://doi.org/10.1130/0091-7613(1989)017<0324:LPTJSM>2.3.CO;2).
- Kent, D.V., Irving, E., 2010. Influence of inclination error in sedimentary rocks on the Triassic and Jurassic apparent pole wander path for North America and implications for Cordilleran tectonics. *J. Geophys. Res. Solid Earth* 115, B10103. <https://doi.org/10.1029/2009JB007205>.
- Kent, D.V., Kjarsgaard, B.A., Gee, J.S., Muttoni, G., Heaman, L.M., 2015. Tracking the late Jurassic apparent (or true) polar shift in U-Pb-dated kimberlites from cratonic North America (Superior Province of Canada). *Geochem. Geophys. Geosyst.* 16, 983–994. <https://doi.org/10.1002/2015GC005734>.
- Kern, H.P., Lavina, E.L.C., Paim, P.S.G., Girelli, T.J., Lana, C., 2021. Paleogeographic evolution of the southern Paraná Basin during the Late Permian and its relation to the Gondwanides. *Sediment. Geol.* 415, 105808 <https://doi.org/10.1016/j.sedgeo.2020.105808>.
- Kirschvink, J.L., 1980. The least-squares line and plane and the analysis of palaeomagnetic data. *Geophys. J. Int.* 62, 699–718. <https://doi.org/10.1111/j.1365-246X.1980.tb02601.x>.
- Kloster, A.C., Gnaedinger, S.C., 2018. Coniferous wood of Agathoxylon from the La Matilde Formation, (Middle Jurassic), Santa Cruz, Argentina. *J. Paleontol.* 92, 546–567. <https://doi.org/10.1017/jpa.2017.145>.
- Kohan Martínez, M., Iglesia Llanos, M.P., Kietzmann, D.A., 2019. Magnetostratigraphy of the Vaca Muerta Formation (Upper Jurassic - Lower Cretaceous) at the Puerta Curaco Section, Neuquén Basin, Argentina, in: Resúmenes. Presented at the VII SIMPOSIO ARGENTINO DEL JURÁSICO, Buenos Aires, p. 12.
- König, M., Jokat, W., 2006. The Mesozoic breakup of the Weddell Sea. *J. Geophys. Res. Solid Earth* 111. <https://doi.org/10.1029/2005JB004035>.
- Kulakov, E.V., Torsvik, T.H., Doubrovine, P.V., Slagstad, T., Ganerød, M., Silkose, P., Werner, S.C., 2021. Jurassic fast polar shift rejected by a new high-quality paleomagnetic pole from Southwest Greenland. *Gondwana Res.* 97, 240–262. <https://doi.org/10.1016/j.gr.2021.05.021>.
- Leanza, A.F., 1958. Geología Regional. In: *La Argentina. Suma de Geografía*. Editorial Peuser, Buenos Aires, pp. 217–249.
- Lesta, P.J., Ferello, R., 1972. Región extraandina de Chubut y norte de Santa Cruz. In: Simposio de Geología Regional Argentina. Academia Nacional de Ciencias de Córdoba, Córdoba, pp. 601–653.
- Lossada, A.C., Rapalini, A., Sánchez Betucci, L., 2014. Enjambre de diques básicos de Nico Pérez – Zapicán, Uruguay: evidencias radimétricas y paleomagnéticas sobre su edad. *Rev. Asoc. Geol. Argent.* 71, 345–355.
- Lovecchio, J.P., Rohais, S., Joseph, P., Bolatti, N.D., Ramos, V.A., 2020. Mesozoic rifting evolution of SW Gondwana: a poly-phased, subduction-related, extensional history responsible for basin formation along the Argentinean Atlantic margin. *Earth Sci. Rev.* 203, 103138 <https://doi.org/10.1016/j.earscirev.2020.103138>.
- Macdonald, D., Gomez-Perez, I., Franzese, J., Spalletti, L., Lawver, L., Gahagan, L., Dalziel, I., Thomas, C., Trewin, N., Hole, M., Paton, D., 2003. Mesozoic break-up of SW Gondwana: implications for regional hydrocarbon potential of the southern South Atlantic. *Mar. Pet. Geol.* 20, 287–308. [https://doi.org/10.1016/S0264-8172\(03\)00045-X](https://doi.org/10.1016/S0264-8172(03)00045-X).
- Marshall, J.E.A., 1994. The Falkland Islands: a key element in Gondwana paleogeography. *Tectonics* 13, 499–514. <https://doi.org/10.1029/93TC03468>.
- Martin, A.K., 2007. Gondwana breakup via double-saloon-door rifting and seafloor spreading in a backarc basin during subduction rollback. *Tectonophysics* 445, 245–272. <https://doi.org/10.1016/j.tecto.2007.08.011>.
- Martino, F.D., Paez, G., Echeveste, H., Jovic, S., Tessone, M.O.R., 2020. Felsic magma-water interaction in shallow intrusive environments: timing between fluidal peperites and intrusive hyaloclastites in a jurassic cryptodome from the eastern Deseado Massif (Patagonia, Argentina). *J. S. Am. Earth Sci.* 101, 102654 <https://doi.org/10.1016/j.james.2020.102654>.
- Marzoli, A., Renne, P.R., Piccirillo, E.M., Ernesto, M., Bellieni, G., Min, A.D., 1999. Extensive 200-Million-Year-Old Continental Flood Basalts of the Central Atlantic Magmatic Province. *Science* 284, 616–618. <https://doi.org/10.1126/science.284.5414.616>.
- Matthews, S.J., Atampiz, M., Omar, J.R., Valencia, V., Pérez de Arce, C., Bustos, A., Llona, F., Rodríguez, M.E., Munizaga, W., di Caro, J., Gonzalez, J., Cingolani, C.A., 2021. Lower to Middle Jurassic volcanism and Au–Ag mineralization at Cerro Moro District, Deseado Massif, Argentine Patagonia. *J. S. Am. Earth Sci.* 103622 <https://doi.org/10.1016/j.james.2021.103622>.
- May, P.R., 1971. Pattern of Triassic-Jurassic Diabase Dikes around the North Atlantic in the Context of Predrift Position of the Continents. *Bull. Geol. Soc. Am.* 82, 1285. [https://doi.org/10.1130/0016-7606\(1971\)82\[1285:POTDDA\]2.0.CO;2](https://doi.org/10.1130/0016-7606(1971)82[1285:POTDDA]2.0.CO;2).
- McFadden, P.L., 1990. A new fold test for palaeomagnetic studies. *Geophys. J. Int.* 103, 163–169. <https://doi.org/10.1111/j.1365-246X.1990.tb01761.x>.
- McFadden, P.L., McElhinny, M.W., 1990. Classification of the reversal test in palaeomagnetism. *Geophys. J. Int.* 103, 725–729. <https://doi.org/10.1111/j.1365-246X.1990.tb05683.x>.
- Mena, M., Goguitchaichvili, A., Solano, M.C., Vilas, J.F., 2011. Paleosecular variation and absolute geomagnetic paleointensity records retrieved from the early cretaceous Posadas Formation (Misiones, Argentina). *Stud. Geophys. Geod.* 55, 279. <https://doi.org/10.1007/s11200-011-0016-3>.
- Mirzaei, M., Housen, B.A., Burmester, R.F., Foreman, B.Z., 2021. Paleomagnetic results from Upper Triassic and Middle Jurassic strata of east-Central New Mexico, and implication for North American apparent polar wander path. *Tectonophysics* 811, 228872. <https://doi.org/10.1016/j.tecto.2021.228872>.
- Mizusaki, A.M.P., Thomaz-Filho, A., Milani, E.J., de Césaro, P., 2002. Mesozoic and Cenozoic igneous activity and its tectonic control in northeastern Brazil. *J. S. Am. Earth Sci.* 15, 183–198. [https://doi.org/10.1016/S0895-9811\(02\)00014-7](https://doi.org/10.1016/S0895-9811(02)00014-7).
- Moreira, P., Echeveste, H., Fernández, R., Hartmann, L., Santos, J., 2006. Ajuste geocronológico de la Formación Chon Aike y mineralizaciones epitermales asociadas

- mediante determinaciones isotópicas U-Pb SHRIMP en circones. In: XI Congreso Geológico Chileno. Presented at the Geología Económica, Antofagasta, pp. 311–314.
- Moreira, P., Echeveste, H., Fernández, R., Hartmann, L.A., Santos, J.O.S., Schalamuk, I., 2009. Depositional age of Jurassic epithermal gold-silver ore in the Deseado Massif, Patagonia, Argentina, based on Manantial Espejo and La Josefina prospects. *N. Jb. Geol. Paläont. (Abh.)* 253, 25–40.
- Moreira, P., Fernández, R., Hervé, F., Fanning, C.M., Schalamuk, I.A., 2013. Detrital zircons U-Pb SHRIMP ages and provenance of La Modesta Formation, Patagonia Argentina. *J. S. Am. Earth Sci.* 47, 32–46. <https://doi.org/10.1016/j.jsames.2013.05.010>.
- Muller, V.A.P., Calderón, M., Fodick, J.C., Ghiglione, M.C., Cury, L.F., Massonne, H.-J., Fanning, C.M., Warren, C.J., Ramírez de Arellano, C., Sternai, P., 2021. The closure of the Rocas Verdes Basin and early tectono-metamorphic evolution of the Magallanes Fold-and-Thrust Belt, southern Patagonian Andes (52–54°S). *Tectonophysics* 798, 228686. <https://doi.org/10.1016/j.tecto.2020.228686>.
- Muttoni, G., Kent, D.V., 2019. Jurassic monster polar shift confirmed by sequential paleopoles from Adria, Promontory of Africa. *J. Geophys. Res. Solid Earth* 0. <https://doi.org/10.1029/2018JB017199>.
- Navarrete, C., 2021. The volcanism of the Jurassic Chon Aike Silicic LIP influenced by Paleozoic inherited crustal structures in the northeastern Deseado Massif, Patagonia. *J. S. Am. Earth Sci.* 112, 103611. <https://doi.org/10.1016/j.jsames.2021.103611>.
- Navarrete, C., Gianni, G., Encinas, A., Márquez, M., Kamerbeek, Y., Valle, M., Folguera, A., 2019. Triassic to Middle Jurassic geodynamic evolution of southwestern Gondwana: from a large flat-slab to mantle plume suction in a rollback subduction setting. *Earth Sci. Rev.* 194, 125–159. <https://doi.org/10.1016/j.earscirev.2019.05.002>.
- Navarrete, C., Butler, K.L., Hurley, M., Márquez, M., 2020. An early Jurassic graben caldera of Chon Aike silicic LIP at the southernmost massif of the world: the Deseado caldera, Patagonia, Argentina. *J. S. Am. Earth Sci.* 101, 102626. <https://doi.org/10.1016/j.jsames.2020.102626>.
- Navarrete, C., Hurley, M., Butler, K., Liendo, I., Litvak, V., Folguera, A., 2021. Jurassic volcanism of the Chon Aike Silicic LIP in the northeastern Deseado Massif. *J. S. Am. Earth Sci.* 107, 102886. <https://doi.org/10.1016/j.jsames.2020.102886>.
- Nomade, S., Théveniaut, H., Chen, Y., Pouclet, A., Rigollet, C., 2000. Paleomagnetic study of French Guyana Early Jurassic dolerites: hypothesis of a multistage magmatic event. *Earth Planet. Sci. Lett.* 184, 155–168. [https://doi.org/10.1016/S0012-821X\(00\)00305-8](https://doi.org/10.1016/S0012-821X(00)00305-8).
- Nomade, S., Knight, K.B., Beutel, E., Renne, P.R., Verati, C., Féraud, G., Marzoli, A., Youbi, N., Bertrand, H., 2007. Chronology of the Central Atlantic Magmatic Province: Implications for the Central Atlantic rifting processes and the Triassic–Jurassic biotic crisis. *Palaeogeogr. Palaeoclimatol. Palaeoecol.*, Triassic–Jurassic Boundary events: problems, progress, possibilities 244, 326–344. <https://doi.org/10.1016/j.palaeo.2006.06.034>.
- Nürnberg, D., Müller, R.D., 1991. The tectonic evolution of the South Atlantic from late Jurassic to present. *Tectonophysics* 191, 27–53. [https://doi.org/10.1016/0040-1951\(91\)90231-G](https://doi.org/10.1016/0040-1951(91)90231-G).
- Páez, G.N., Ruiz, R., Guido, D.M., Ríos, F.J., Subias, I., Recio, C., Schalamuk, I.B., 2016. High-grade ore shoots at the Martha epithermal vein system, Deseado Massif, Argentina: the interplay of tectonic, hydrothermal and supergene processes in ore genesis. *Ore Geol. Rev.* 72, 546–561. <https://doi.org/10.1016/j.oregeorev.2015.07.026>.
- Pankhurst, R.J., Rapela, C.R., 1995. Production of Jurassic rhyolite by anatexis of the lower crust of Patagonia. *Earth Planet. Sci. Lett.* 134, 23–36. [https://doi.org/10.1016/0012-821X\(95\)00103-J](https://doi.org/10.1016/0012-821X(95)00103-J).
- Pankhurst, R., Rapela, C., Márquez, M., 1993. Geocronología y petrogénesis de los granitoides Jurásicos del norte del Macizo del Desesado. In: Actas. Presented at the XII Congreso Geológico Argentino, Asociación Geológica Argentina, Buenos Aires, pp. 134–141.
- Pankhurst, R.J., Riley, T.R., Fanning, C.M., Kelley, S.P., 2000. Episodic Silicic Volcanism in Patagonia and the Antarctic Peninsula: Chronology of Magmatism Associated with the Break-up of Gondwana. *J. Pet.* 41, 605–625. <https://doi.org/10.1093/petrology/41.5.605>.
- Pankhurst, R.J., Rapela, C.W., Loske, W.P., Márquez, M., Fanning, C.M., 2003. Chronological study of the pre-Permian basement rocks of southern Patagonia. *J. S. Am. Earth Sci.* 16, 27–44. [https://doi.org/10.1016/S0895-9811\(03\)00017-8](https://doi.org/10.1016/S0895-9811(03)00017-8). The Pacific Gondwana margin SI.
- Panza, J.L., 1982. Descripción geológica de las Hojas 53e «Gobernador Moyano» y 54e «Cerro Vanguardia», Inédito. ed. Dirección Nacional de Minería y Geología, Buenos Aires.
- Panza, J.L., 1984. Descripción geológica de las Hojas 54f «Bajo de la Leona» y 54g «Bahía Laura», provincia de Santa Cruz, Inédito. ed. Dirección Nacional de Minería y Geología, Buenos Aires.
- Panza, J.L.A., Márquez, M.J., 1994. Hoja Geológica 4966-I / II Bahía Laura. Servicio Geológico Minero Argentino, Instituto de Geología y Recursos Minerales.
- Panza, J.L.A., Irigoyen, M.V., Genini, A., 1994a. Hoja Geológica 4969-IV Puerto San Julián. Servicio Geológico Minero Argentino, Instituto de Geología y Recursos Minerales.
- Panza, J.L.A., Marín, G., Zubía, M.A., 1998. Hoja Geológica 4969-I Gobernador Gregores. Servicio Geológico Minero Argentino, Instituto de Geología y Recursos Minerales.
- Panza, J.L.A., Cobos, J.C., Zubía, M.A., Franchi, M., 2001a. Hoja Geológica 4769-III Destacamento La María. Servicio Geológico Minero Argentino, Instituto de Geología y Recursos Minerales.
- Panza, J.L.A., Genini, A., Franchi, M., 2001b. Hoja Geológica 4769-IV Monumento Natural Bosques Petrificados. Servicio Geológico Minero Argentino, Instituto de Geología y Recursos Minerales.
- Panza, J.L.A., Cobos, J.C., Asato, C.G., Candaosa, N.G., Chavez, S.B., Gambadé Álvarez, M.L., Olmos, M.I., Tavítian Serrano, A.F., 2003. Mapa Geológico de la Provincia de Santa Cruz. Servicio Geológico Minero Argentino. Instituto de Geología y Recursos Minerales.
- Panza, J.L.A., Sacomani, L.E., Giacosa, R.E., Franchi, M., 2018. Hoja Geológica 4972-II Lago Cardiel. Servicio Geológico Minero Argentino. Instituto de Geología y Recursos Minerales.
- Panza, J.L.A., Zubía, M.A., Godeas, M.C., 1994b. Hoja Geológica 4969-II Tres Cerros. Servicio Geológico Minero Argentino. Instituto de Geología y Recursos Minerales.
- Pezzi, E.E., 1970. Informe geológico preliminar zona Los Pirineos-Cañadón Largo. (Inédito No. Permiso Ya GSC 74). Yacimientos Petrolíferos Fiscales.
- Ramos, V.A., 1999. Las provincias geológicas del territorio argentino. In: *Geología Argentina*. Instituto de Geología y Recursos Minerales, Buenos Aires, pp. 41–96.
- Ramos, V.A., 2008. Patagonia: A paleozoic continent adrift? *J. S. Am. Earth Sci.* 26, 235–251. <https://doi.org/10.1016/j.jsames.2008.06.002>.
- Rapalini, A.E., Lopez de Luchi, M., 2000. Paleomagnetism and magnetic fabric of Middle Jurassic dykes from Western Patagonia, Argentina. *Phys. Earth Planet. Inter.* 120, 11–27. [https://doi.org/10.1016/S0031-9201\(00\)00140-0](https://doi.org/10.1016/S0031-9201(00)00140-0).
- Rapela, C.W., Pankhurst, R.J., 1992. The granites of northern Patagonia and the Gaster Fault System in relation to the break-up of Gondwana. *Geol. Soc. Spec. Publ.* 68, 209–220. <https://doi.org/10.1144/GSL.SP.1992.068.01.13>.
- Rapela, C., Pankhurst, R., 1993. El volcanismo riolítico del noreste de la Patagonia: un evento meso-Jurásico de corta duración y origen profundo. In: *Actas. Presented at the XII Congreso Geológico Argentino, Asociación Geológica Argentina, Buenos Aires*, pp. 179–188.
- Raposo, M.I.B., Ernesto, M., 1995. An early cretaceous paleomagnetic pole from Ponta Grossa dikes (Brazil): Implications for the South American Mesozoic apparent polar wander path. *J. Geophys. Res. Solid Earth* 100, 20095–20109. <https://doi.org/10.1029/95JB01681>.
- Reimer, W., Miller, H., Mehl, H., 1996. Mesozoic and Cenozoic palaeo-stress fields of the South Patagonian Massif deduced from structural and remote sensing data. *Geol. Soc. Spec. Publ.* 108, 73–85. <https://doi.org/10.1144/GSL.SP.1996.108.01.06>.
- Renda, E.M., Alvarez, D., Prezzi, C., Oriolo, S., Vizán, H., 2019. Inherited basement structures and their influence in foreland evolution: a case study in Central Patagonia, Argentina. *Tectonophysics* 772, 228232. <https://doi.org/10.1016/j.tecto.2019.228232>.
- Renne, P.R., Ernesto, M., Pacca, I.G., Coe, R.S., Glen, J.M., Prévot, M., Perrin, M., 1992. The age of Paraná flood volcanism, rifting of Gondwanaland, and the Jurassic–cretaceous Boundary. *Science* 258, 975–979. <https://doi.org/10.1126/science.258.5084.975>.
- Renne, P.R., Deckart, K., Ernesto, M., Fe'raud, G., Piccirillo, E.M., 1996. Age of the Ponta Grossa dike swarm (Brazil), and implications to Paraná flood volcanism. *Earth Planet. Sci. Lett.* 144, 199–211. [https://doi.org/10.1016/0012-821X\(96\)00155-0](https://doi.org/10.1016/0012-821X(96)00155-0).
- Riel, N., Jaillard, E., Martelat, J.-E., Guillot, S., Braun, J., 2018. Permian-Triassic Tethyan realm reorganization: implications for the outward Pangea margin. *J. S. Am. Earth Sci.* 81, 78–86. <https://doi.org/10.1016/j.jsames.2017.11.007>.
- Riley, T.R., Jordan, T.A., Leat, P.T., Curtis, M.L., Millar, I.L., 2020. Magmatism of the Weddell Sea rift system in Antarctica: Implications for the age and mechanism of rifting and early stage Gondwana breakup. *Gondwana Res.* 79, 185–196. <https://doi.org/10.1016/j.gr.2019.09.014>.
- Ronda, G., Ghiglione, M.C., Barberón, V., Coutand, I., Tobal, J., 2019. Mesozoic – Cenozoic evolution of the Southern Patagonian Andes fold and thrust belt (47°–48°S): Influence of the Rocas Verdes basin inversion and onset of Patagonian glaciations. *Tectonophysics* 765, 83–101. <https://doi.org/10.1016/j.tecto.2019.05.009>.
- Ruiz González, V., Puigdomenech, C.G., Renda, E.M., Boltshauser, B., Somoza, R., Vizán, H., Zaffarana, C.B., Taylor, G.K., Haller, M., Fernández, R., 2019. New paleomagnetic pole for the Upper Jurassic Chon Aike Formation of southern Argentina (South America): Testing the tectonic stability of Patagonia with respect to South America, and implications to Middle Jurassic–early cretaceous true polar wander. *Tectonophysics* 750, 45–55. <https://doi.org/10.1016/j.tecto.2018.10.028>.
- Ruiz González, V., Puigdomenech, C.G., Zaffarana, C.B., Vizán, H., Somoza, R., 2020. Paleomagnetic evidence of the brittle deformation of the Central Patagonian Batholith at Gaster area (Chubut Province, Argentina). *J. S. Am. Earth Sci.* 98, 102442. <https://doi.org/10.1016/j.jsames.2019.102442>.
- Schult, A., Guerreiro, S.D.C., 1979. Palaeomagnetism of Mesozoic igneous rocks from the Maranhão Basin, Brazil, and the time of opening of the South Atlantic. *Earth Planet. Sci. Lett.* 42, 427–436. [https://doi.org/10.1016/0012-821X\(79\)90051-7](https://doi.org/10.1016/0012-821X(79)90051-7).
- Seitz, S., Pütlitz, B., Baumgartner, L.P., Bouvier, A.-S., 2018. The role of crustal melting in the formation of rhyolites: Constraints from SIMS oxygen isotope data (Chon Aike Province, Patagonia, Argentina). *Am. Mineral.* 103, 2011–2027. <https://doi.org/10.2138/am-2018-6520>.
- Somoza, R., Zaffarana, C.B., 2008. Mid-Cretaceous polar standstill of South America, motion of the Atlantic hotspots and the birth of the Andean cordillera. *Earth Planet. Sci. Lett.* 271, 267–277. <https://doi.org/10.1016/j.epsl.2008.04.004>.
- Somoza, R., Vizán, H., Taylor, G.K., 2008. Tectonic rotations in the Deseado Massif, southern Patagonia, during the breakup of Western Gondwana. *Tectonophysics* 460, 178–185. <https://doi.org/10.1016/j.tecto.2008.08.004>.
- Souza, Z.S., Vasconcelos, P.M., Nascimento, M.A.L., Silveira, F.V., Paiva, H.S., Dias, L.G. S., Thiede, D., Carmo, I.O., 2003. 40Ar/39Ar geochronology of Mesozoic and Cenozoic magmatism in NE Brazil. In: *Short Papers of the IV South American Symposium on Isotope Geology*, p. 4.
- Sruoga, P., Palma, M.A., 1984. La Formación Chon Aike en su área clásica de afloramientos. In: *Actas. Presented at the 9º Congreso Geológico Argentino, Asociación Geológica Argentina*, pp. 171–184.

- Sruoga, P., Palma, M.A., 1986. Los domos riolíticos jurásicos de los cerros Laciar, Moro, Baguales y La Pava, Departamento Deseado, provincia de Santa Cruz. Rev. Asoc. Geol. Argent. 3–4, 397–401.
- Sruoga, P., Busteros, A., Giacosa, R., Martínez, H., Kleiman, L., Japas, S., Maloberti, A., Gayone, M.R., 2008. Análisis litofacial y estructural del complejo volcánico Bahía Laura en el área El Dorado-Monserrat, provincia de Santa Cruz. Rev. Asoc. Geol. Argent. 63, 653–664.
- Stewart, K., Turner, S., Kelley, S., Hawkesworth, C., Kirstein, L., Mantovani, M., 1996. 3-D, 40Ar-39Ar geochronology in the Paraná continental flood basalt province. Earth Planet. Sci. Lett. 143, 95–109. [https://doi.org/10.1016/0012-821X\(96\)00132-X](https://doi.org/10.1016/0012-821X(96)00132-X).
- Stipanicic, P.N., Reig, 1955. Breve noticia sobre el hallazgo de anuros en el denominado Complejo Porfírico de la Patagonia Extraandina, con consideraciones acerca de la composición geológica del mismo. Rev. Asoc. Geol. Argent. 215–233.
- Stipanicic, P.N., Reig, O.A., 1957. El “Complejo porfírico de la Patagonia Extraandina” y su fauna de anuros. In: Acta Geologica Lilloana, Tucumán.
- Storey, B.C., Alabaster, T., Hole, M.J., Pankhurst, R.J., Wever, H.E., 1992. Role of subduction-plate boundary forces during the initial stages of Gondwana break-up: evidence from the proto-Pacific margin of Antarctica. Geol. Soc. Spec. Publ. 68, 149–163. <https://doi.org/10.1144/GSL.SP.1992.068.01.10>.
- Suárez, R.J., Ghiglione, M.C., Calderón, M., Sue, C., Martinod, J., Guillaume, B., Rojo, D., 2019. The metamorphic rocks of the Nunatak Viedma in the Southern Patagonian Andes: Provenance sources and implications for the early Mesozoic Patagonia-Antarctic Peninsula connection. J. S. Am. Earth Sci. 90, 471–486. <https://doi.org/10.1016/j.jsames.2018.12.015>.
- Torsvik, T.H., Müller, R.D., der Voo, R.V., Steinberger, B., Gaina, C., 2008. Global plate motion frames: toward a unified model. Rev. Geophys. 46 <https://doi.org/10.1029/2007RG000227>.
- Torsvik, T.H., Rousse, S., Labails, C., Smethurst, M.A., 2009. A new scheme for the opening of the South Atlantic Ocean and the dissection of an Aptian salt basin. Geophys. J. Int. 177, 1315–1333. <https://doi.org/10.1111/j.1365-246X.2009.04137.x>.
- Torsvik, T.H., Van der Voo, R., Preeden, U., Mac Niocaill, C., Steinberger, B., Doubrovine, P.V., with Hinsbergen, D.J.J., Domeier, M., Gaina, C., Tohver, E., Meert, J.G., McCausland, P.J.A., Cocks, L.R.M., 2012. Phanerozoic polar wander, palaeogeography and dynamics. Earth Sci. Rev. 114, 325–368. <https://doi.org/10.1016/j.earscirev.2012.06.007>.
- Torsvik, T.H., Steinberger, B., Shephard, G.E., Doubrovine, P.V., Gaina, C., Domeier, M., Conrad, C.P., Sager, W.W., 2019. Pacific-Panthalassic Reconstructions: Overview, Errata and the Way Forward. Geochem. Geophys. Geosyst. 20, 3659–3689. <https://doi.org/10.1029/2019GC008402>.
- Turic, M.A., 1969. Perfiles estratigráficos al sur del curso medio del río Deseado, entre Punta España y Meseta Baqueró, provincia de Santa Cruz (Inédito). Yacimientos Petrolíferos Fiscales, Buenos Aires.
- Turner, S., Regelous, M., Kelley, S., Hawkesworth, C., Mantovani, M., 1994. Magmatism and continental break-up in the South Atlantic: high precision 40Ar-39Ar geochronology. Earth Planet. Sci. Lett. 121, 333–348. [https://doi.org/10.1016/0012-821X\(94\)90076-0](https://doi.org/10.1016/0012-821X(94)90076-0).
- Uliana, M.A., Biddle, K.T., 1987. Permian to late Cenozoic Evolution of Northern Patagonia: main tectonic events, Magmatic activity, and depositional trends. In: Gondwana Six: Structure, Tectonics, and Geophysics. American Geophysical Union (AGU), pp. 271–286. <https://doi.org/10.1029/GM040p0271>.
- Uliana, M.A., Biddle, K.T., 1988. Mesozoic-Cenozoic paleogeographic and geodynamic evolution of southern South America. Rev. Bras. Geoscienc. 18, 172–190.
- Valencio, D.A., Vilas, J.F., 1970. Palaeomagnetism of some Middle Jurassic Lavas from South-east Argentina. Nature 225, 262–264. <https://doi.org/10.1038/225262a0>.
- van de Lagemaat, S.H.A., Swart, M.L.A., Vaes, B., Kosters, M.E., Boschman, L.M., Burton-Johnson, A., Bijl, P.K., Spakman, W., van Hinsbergen, D.J.J., 2021. Subduction initiation in the Scotia Sea region and opening of the Drake Passage: when and why? Earth Sci. Rev. 215, 103551. <https://doi.org/10.1016/j.earscirev.2021.103551>.
- Van der Voo, R., 1990. The reliability of paleomagnetic data. Tectonophys. Reliabil. Paleomag. Data 184, 1–9. [https://doi.org/10.1016/0040-1951\(90\)90116-P](https://doi.org/10.1016/0040-1951(90)90116-P).
- van Hinsbergen, D.J.J., Torsvik, T.H., Schmid, S.M., Matenco, L.C., Maffione, M., Vissers, R.L.M., Gürer, D., Spakman, W., 2019. Orogenic architecture of the Mediterranean region and kinematic reconstruction of its tectonic evolution since the Triassic. Gondwana Res. <https://doi.org/10.1016/j.gr.2019.07.009>.
- Viera, R., Pezzuchi, H., 1976. Presencia de sedimentitas pérmiticas en contacto con rocas del «Complejo metamórfico» de la Patagonia Extrandina, estancia Dos Hermanos, provincia de Santa Cruz. Rev. Asoc. Geol. Argent. 31, 281–283.
- Vilas, J.F.A., 1974. Palaeomagnetism of some igneous rocks of the Middle Jurassic Chon-Aike Formation from Estancia La Reconquist, Province of Santa Cruz, Argentina. Geophys. J. Int. 39, 511–522. <https://doi.org/10.1111/j.1365-246X.1974.tb05469.x>.
- Vizán, H., 1998. Paleomagnetism of the lower Jurassic Lepá and Osta Arena formations. Argentine Patagonia. J. S. Am. Earth Sci. 11, 333–350. [https://doi.org/10.1016/S0895-9811\(98\)00018-2](https://doi.org/10.1016/S0895-9811(98)00018-2).
- Vizán, H., Ixer, R., Turner, P., Cortés, J.M., Cladera, G., 2004. Paleomagnetism of Upper Triassic rocks in the Los Colorados hill section, Mendoza province, Argentina. J. S. Am. Earth Sci. 18, 41–59. <https://doi.org/10.1016/j.jsames.2004.08.008>.
- Vizán, H., Prezzi, C.B., Geuna, S.E., Japas, M.S., Renda, E.M., Franzese, J., Zele, M.A.V., 2017. Paleotethys slab pull, self-lubricated weak lithospheric zones, polooidal and toroidal plate motions, and Gondwana tectonics. Geosphere 13, 1541–1554. <https://doi.org/10.1130/GES01444.1>.
- von Gosen, W., Loske, W., 2004. Tectonic history of the Calcatapul Formation, Chubut province, Argentina, and the “Gastre fault system.”. J. S. Am. Earth Sci. 18, 73–88. <https://doi.org/10.1016/j.jsames.2004.08.007>.
- Wilson, R.L., Dagley, P., McCormack, A.G., 1972. Palaeomagnetic evidence about the source of the Geomagnetic Field. Geophys. J. Int. 28, 213–224. <https://doi.org/10.1111/j.1365-246X.1972.tb06124.x>.
- Zaffarana, C.B., Somoza, R., 2012. Palaeomagnetism and 40Ar/39Ar dating from lower Jurassic rocks in Gastre, Central Patagonia: further data to explore tectonomagmatic events associated with the break-up of Gondwana. J. Geol. Soc. 169, 371–379. <https://doi.org/10.1144/0016-7649-2011-089>.
- Zaffarana, C.B., López de luchi, M.G., Somoza, R., Mercader, R., Giacosa, R., Martino, R., D., 2010. Anisotropy of magnetic susceptibility study in two classical localities of the Gastre Fault System, Central Patagonia. J. S. Am. Earth Sci. 30, 151–166. <https://doi.org/10.1016/j.jsames.2010.10.003>.
- Zaffarana, C.B., Montenegro, T., Somoza, R., 2012. The host rock of the central patagonian batholith in gastre: further insights on the late Triassic to early Jurassic Deformation in the Region. Rev. Asoc. Geol. Argent. 69, 106–126.
- Zaffarana, C.B., Somoza, R., López de Luchi, M., 2014. The late Triassic Central Patagonian Batholith: Magma hybridization, 40Ar/39Ar ages and thermobarometry. J. S. Am. Earth Sci. 55, 94–122. <https://doi.org/10.1016/j.jsames.2014.06.006>.
- Zaffarana, C.B., Somoza, R., Orts, D.L., Mercader, R., Boltshauser, B., Ruiz González, V., Puigdomenech, C., 2017. Internal structure of the late Triassic Central Patagonian batholith at Gastre, southern Argentina: Implications for pluton emplacement and the Gastre fault system. Geosphere 13, 1973–1992. <https://doi.org/10.1130/GES01493.1>.
- Zhong, S., Zhang, N., Li, Z.-X., Roberts, J.H., 2007. Supercontinent cycles, true polar wander, and very long-wavelength mantle convection. Earth Planet. Sci. Lett. 261, 551–564. <https://doi.org/10.1016/j.epsl.2007.07.049>.
- Zijderveld, J.D.A., 1967. A. C. Demagnetization of rocks: analysis of results. In: Collinson, D.W., Creer, K.M., Runcorn, S.K. (Eds.), Developments in Solid Earth Geophysics, Methods in Palaeomagnetism. Elsevier, pp. 254–286. <https://doi.org/10.1016/B978-1-4832-2894-5.50049-5>.